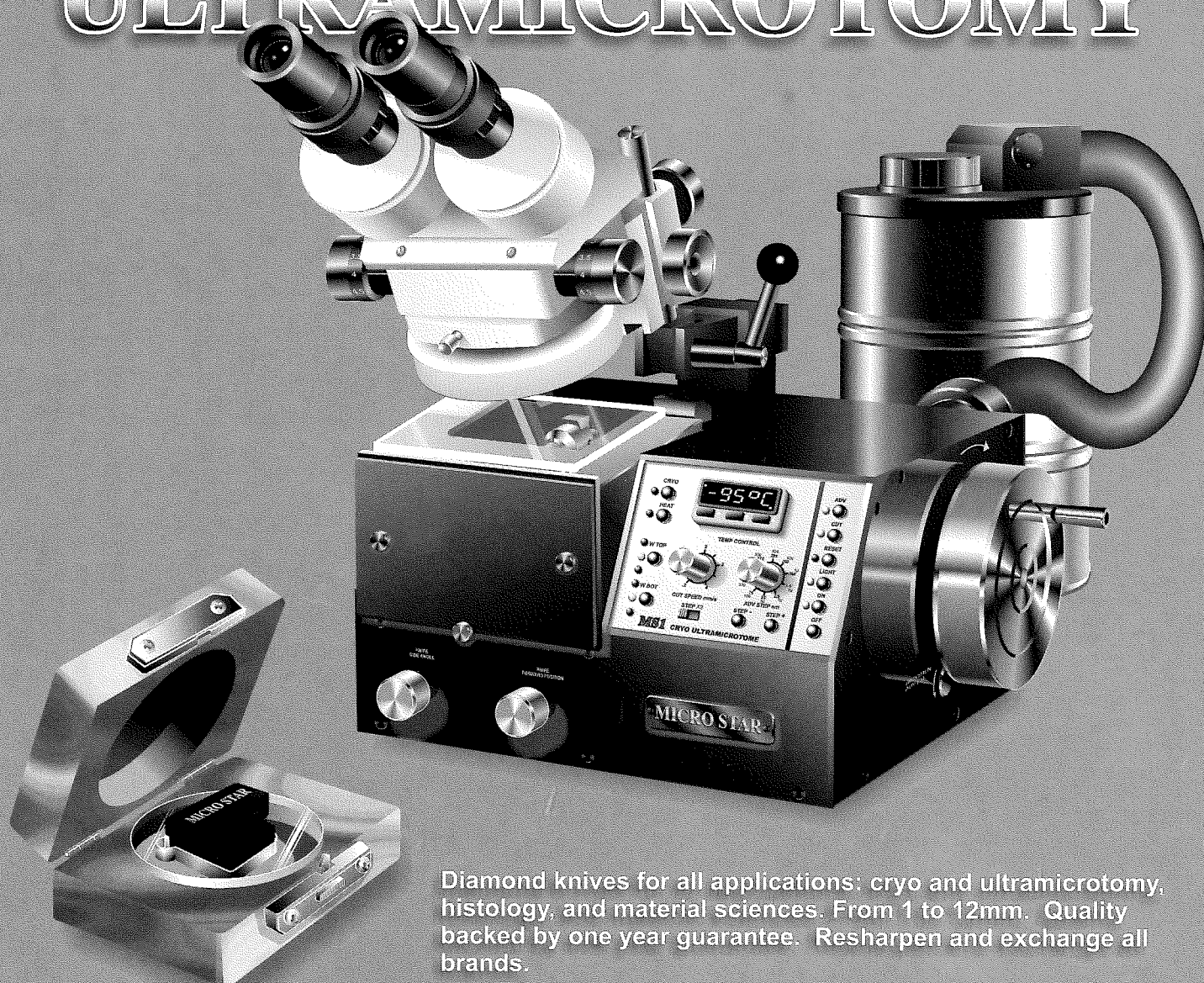


FROST RING ANALYSES

MICRO STAR ULTRAMICROTOMY



Diamond knives for all applications: cryo and ultramicrotomy, histology, and material sciences. From 1 to 12mm. Quality backed by one year guarantee. Resharpen and exchange all brands.

Cryo Ultramicrotome integrated in a single portable instrument. Designed for TEM and SPM sample preparation. Microprocessor controlled cryogenic system. Includes Dewar and complete set of attachments. Sections 25nm to 5 μ , cryo temperatures to -130°C. Fully automatic or manual operation. High precision and stability at a fraction of the cost of other systems.

Request information, manuals and complete price list, or see them at the web.

800 533 2509
FAX 936 294 9861
MICROSTARTECH.COM

MICRO STAR
TECHNOLOGIES

TSM OFFICERS 2004-2005

President:

ANN E. RUSHING
Department of Biology
Baylor University, Waco, Texas 76798-7388
(254) 710-2911 FAX (254) 710-2969
E-mail: Ann_Rushing@baylor.edu

President-elect:

SANDRA WESTMORELAND
Department of Biology
University of Texas at Arlington
Arlington, Texas 76019-0498
E-mail: slwestmoreland@uta.edu

Past President:

PAMELA J. NEILL
R3-24
Alcon Laboratories, Inc.
6201 South Freeway, Fort Worth, Texas 76134-2099
(817) 568-6497
E-mail: pamelaneill@alconlabs.com

Secretary:

ANN S. BURKE
Electron Microscopy Lab
Shriners Hospital for Children
815 Market Street, Galveston, Texas 77550
(409) 770-6653
E-mail: aburke@utmb.edu

Secretary-elect:

ROBERT CHAMPAIGN
Sensors and Electronic Systems
Raytheon Network Centric Systems
2501 W. University, McKinney, Texas 75070
E-mail: r-champaign@raytheon.com

Treasurer:

ROBERT DROLESKEY
USDA/ARS/SPARC
2881 F&B Rd., College Station, Texas 77845
(979) 260-9316 FAX (979) 260-9332
E-mail: droleskey@ffsr.tamu.edu

Treasurer-elect:

MARTHA GRACEY
Department of Biology
University of Texas at Arlington
Arlington, Texas 76019-0498
E-mail: martha@uta.edu

Program Chairman:

SUSAN ROBBINS
Department of Pathology
Baylor College of Medicine
One Baylor Plaza, Rm. 212B, Houston, Texas 77030
(713) 798-4658 FAX (713) 798-3945
E-mail: srobbins@bcm.tmc.edu

Program chair-elect:

JODI ROEPSCH
Electronic Systems
Raytheon Network Centric Systems
2501 W. University, McKinney, Texas 75070
E-mail: j-roepsch2@raytheon.com

APPOINTED OFFICERS

Corporate Member Representative:

Mike Crowley
Oxford Instruments, Inc.
3536 Flora Vista Loop, Round Rock, Texas 78681
(512) 246-7551 FAX (512) 246-7501
E-mail: crowley@ma.oxinst.com

Student Representative:

SAM HO
Transplant Immunology Research Laboratory
Baylor University Medical Center
3409 Worth Street Suite 530, Dallas, Texas 75246
(214) 820-4123
E-mail: Sam_Ho@baylor.edu

TSM Journal Editor:

CAMELIA G.-A. MAIER
Department of Biology
Texas Woman's University, Denton, Texas 76204-5799
(940) 898-2358 FAX (940) 898-2382
E-mail: cmaier@twu.edu

TSM Web Page Master:

BECKY HOLDFORD
Texas Instruments Inc.
13570 North Central Texas Expressway,
MS 3704, Dallas, Texas 75243
(972) 995-2360
E-mail: r-holdford@ti.com

Contents

TEXAS JOURNAL OF MICROSCOPY
VOLUME 35, NUMBER 1, 2004
ISSN 0196-5662



Camelia G.-A. Maier, Editor

Department of Biology, Texas Woman's University, Denton, TX 76204

Official Journal of the Texas Society for Microscopy

"TSM - Embracing all forms of microscopy"

www.texasmicroscopy.org

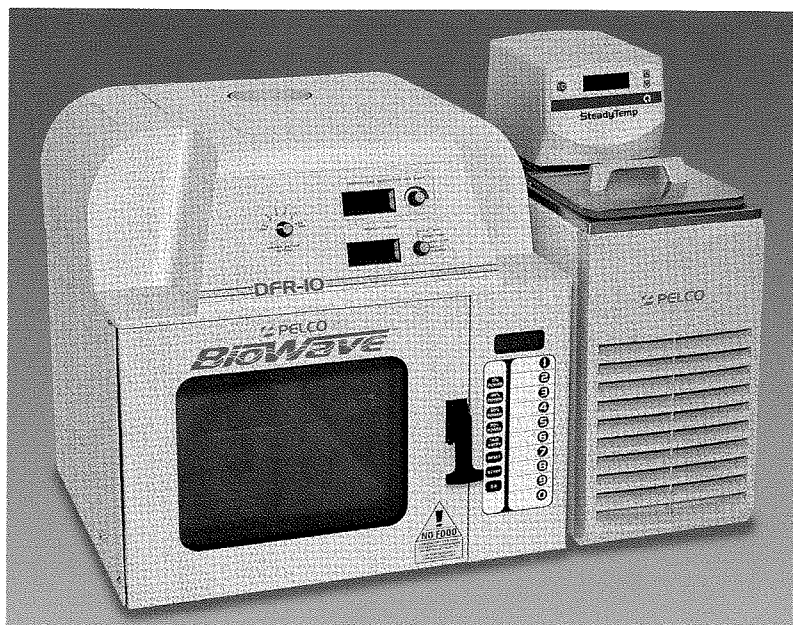
Answer to "What Is It?" from Tex. J. Micros. 34:1	6
Editorial Policy	6
President's Message	7
Treasurer's Reports	9
Abstracts	10
Long Abstracts:	
<i>Fluorescent Microscopy on the BSBMV Infected</i>	
<i>Sugar Beet Foliage</i>	
Nabarun Ghosh, Maria E. Villanueva and Deb Mahapatra	14
<i>Common Failure Modes in SN/PB Solder Joints</i>	
Jodi A. Roepsch	16
<i>XPLORE #D: A Total Solution Package for Electron Tomography</i>	
Linda Melanson	17
Advertiser's Index	17
Our Students	19
Corporate Members	21
Manuscript:	
<i>Assessment of Aeroallergen Concentration in the Atmosphere of</i>	
<i>the Texas Panhandle using a burkard Volumetric Spore Trap</i>	
Nabarun Ghosh, Rene Camacho,	
Constantine K. Saadeh and Michael C. Gaylor	22
What Is It?	27
TSM Application For Membership	30

ON THE COVER

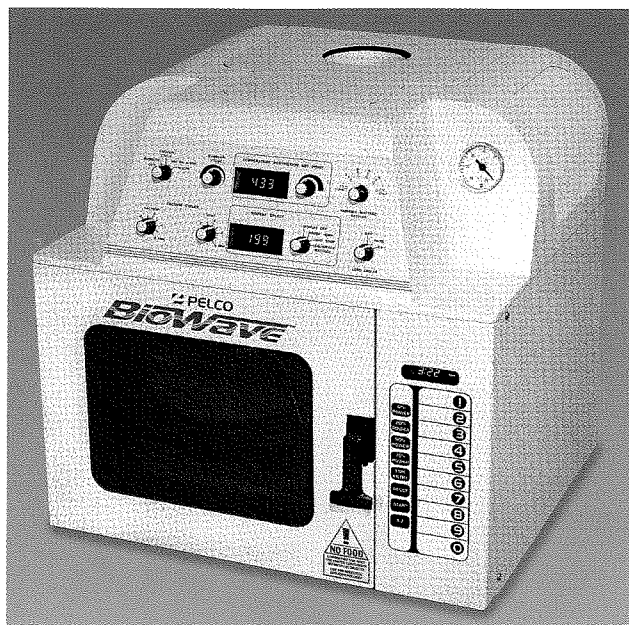
Image analyses techniques for frost ring studies: upper left — **FFT analysis** of normal and frost annual rings in *Pinus longaeva*; upper right — **Line analysis** of tracheid files in *P. longaeva* showing tracheid files and enlarged ray components; lower left — **Isolation analysis** of a group of very distorted frost ring cells in *P. longaeva*; lower right — **File analysis** showing tracheid files as they pass through a very slight frost ring in *P. longaeva*. For more details about the above techniques see the corresponding abstract by **Howard J. Arnott**, (pg. 11) The Department of Biology and The Center for Electron Microscopy, The University of Texas at Arlington, Arlington, Texas 76019.

Venture Into The Now

EM & LM Processing, Immunolabeling, Bone Decalcification



PELCO BioWave® DFR-10 Laboratory Tissue Processing System
For more details: http://www.tedpella.com/34700_html/34800.htm



PELCO BioWave® Laboratory Tissue Processing System
For more details: http://www.tedpella.com/34700_html/34700.htm

PELCO® Microwave Tissue Processors have more than one use

Immunology, Neurosciences, Diagnostic EM, Histology, Botany, Pharmacology and Biology are some of the fields of application. Your routine tissue processing or special investigatory trials invite methods that can improve final results and speed your work.

Variables offered by the PELCO® models, which may be adjusted to get optimum results are:

- | | |
|----------------------------|--|
| Low Temperature Processing | The only laboratory microwave system that does not rely on heating protocols but rather application of microwave energy with heat removal to optimize results |
| True Variable Power | Several power levels may be selected to give 100% of that level during a time period; this means full control and constant application of power even at low wattages |
| PELCO ColdSpot® | A patented, effective method to hold a flat area in the processor at a certain temperature level. No hot or cold spots to "locate" |
| Vacuum | The 3435 PELCO® EM MW Vacuum Chamber holds vacuum down to 1 torr (1mm Hg, 1.33mBar) |
| Cooler than Ambient | Our PELCO SteadyTemp™ will permit temperatures below ambient to be run through the PELCO ColdSpot® |

Other operating and safety features are included. Call or email for more information.

 **TED PELLA, INC.**
Microscopy Products for Science and Industry

4595 Mountain Lakes Blvd., Redding, CA 96003-1448 • Phone: 530-243-2200 or 800-237-3526 (USA)
FAX: 530-243-3761 • Email: sales@tedpella.com • Web Site: <http://www.tedpella.com>

SteadyTemp is a trademark and PELCO, PELCO BioWave and PELCO ColdSpot are registered trademarks of Ted Pella, Inc. All rights reserved.
©Ted Pella, Inc., 03-04.

TRUST

Your Instincts. Your Research.
Our *NEW* Equipment.



EMS 9000
Precision Pulsed Laboratory
Microwave Oven
...with load cooler and
vacuum processor



EMS 5000
Oscillating Tissue Slicer
...for the most challenging
sectioning—as thin as
five microns



TriPix
Advanced Digital Camera Systems
...available in RGB, IR and Spectral versions

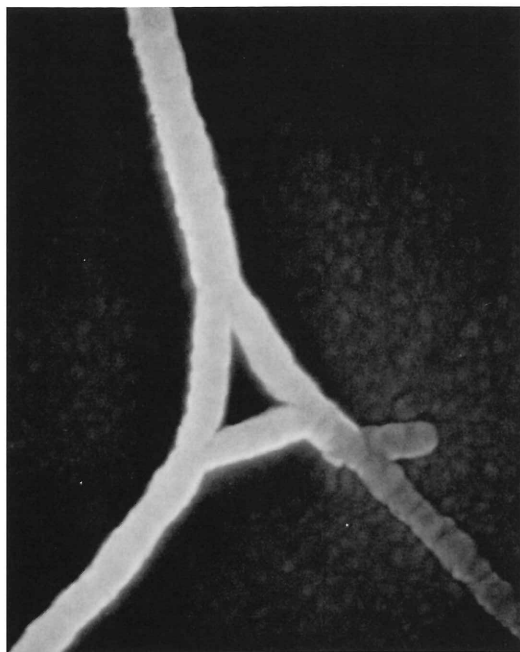
Brand New State-of-the-Art Products from THE
Leading Innovator in Electron Microscopy.

**Electron
Microscopy
Sciences**

For more information and a complete catalog, write or call:
321 Morris Road, P.O. Box 251, Fort Washington, PA 19034
(215) 646-1566 • (800) 523-5874 • Fax (215) 646-8931
email: sgkcc@aol.com • <http://www.emsdiasum.com>

Answer to "What Is It?"

from Texas Journal of Microscopy 34:1



Scanning electron micrograph illustrating fused flagella of *Campylobacter jejuni*, by Bob Droleskey, USDA/ARS/SPARC, College Station, Texas 77845. When grown on solid media, such as Campy Cefex Agar, the flagella of multiple *C. jejuni* organisms are frequently observed to be interconnected. As illustrated here, three flagella from three different organisms are fused at a central point. This phenomenon is most likely an artifact induced by fixation of organisms grown on solid media as fused flagella are never observed with broth cultured bacteria.

EDITORIAL POLICY

LETTERS TO THE EDITOR

Letters to the editor are printed as they are received in the order of their arrival. These letters reflect the opinion of the individual TSM member and do not necessarily reflect the opinions of the Editor or the Society. The content of the letters should be concerned with the philosophical or operational aspects of the TSM, the Journal and its contents, academic or national policies as they apply to TSM and/or its members and microscopy in general. Editorial privilege may be evoked to insure that the LETTERS SECTION will neither be used as a political forum nor violate the memberships' trust.

MICROGRAPHS AND COVER PHOTOS

Micrographs submitted for cover photos should be marked as such. The choice of photographs will be made by the Editor. Photograph receipt and/or dispensation will be acknowledged. Photographs will not be returned. Electron micrographs to be used for cover photos and text fillers are welcome and should be selected with some attention to aesthetic appeal as well as excellence both in technique and in scientific information content.

EMPLOYMENT OPPORTUNITIES

The JOB OPPORTUNITIES section will be comprised of a "Jobs Available" and a "Jobs Wanted" sub-sections. Anonymity of individuals listing in the Jobs Wanted or Jobs Available sub-sections may be maintained by correspondence routed through the Editor's office.

TECHNICAL SECTION

The Technical Section will publish TECHNIQUES PAPERS, and HELPFUL HINTS. The TECHNIQUE PAPERS will describe new or improved methods for existing techniques and give examples of the results obtained with methods. The format of the Technique Papers will be the same as that used for regular research reports. HELPFUL HINTS will be in the form of a brief report with an accompanying illustration, if required for clarity. Helpful Hints should embody techniques which will improve or expedite processes and/or procedures used in EM.

PUBLICATION PRIVILEGES

The right to publish Abstracts in the TEXAS JOURNAL OF MICROSCOPY is restricted to TSM members or to those whose membership is pending. A membership application form can usually be found in each issue of the TEXAS JOURNAL OF MICROSCOPY. Membership dues are as follows: student \$10.00; regular members \$30.00; Corporate members \$300.00. Research articles are accepted from both members and non-members. Individuals who belong to TSM by virtue of a corporate membership are invited to participate in Journal submissions as are our regular or student members. However, papers of a commercial nature, either stated or implied, will not be accepted for publication as a Research Report or Techniques Paper. Such papers may be acceptable as advertising copies.

President's Message

I am honored to be serving again as your president. The Texas Society for Microscopy has been a supportive presence in my professional career for many years. I pledge my continued efforts to strengthen the society. I would like to thank the members of the executive committee for their hard work during the past year. Pamela Neill, our Past-President, navigated us toward the future during her time as president and I hope to keep us moving on a pathway forward.

Congratulations to those who are accepting leadership roles in the society. The society has reached a critical point when we all must be recruiting new members and encouraging the active participation of our colleagues. We need a new generation of microscopists to become involved in society activities. During the past two years, I have contacted colleges and universities around the state encouraging their participation and will continue with these efforts. I challenge each of you to invite your colleagues at your home institution and around the state to attend a meeting and experience the supportive environment we provide for students. I also encourage you to present your own research and to consider publishing in the Texas Journal of Microscopy.

Our last gathering, in conjunction with the 2003 Microscopy & Microanalysis meeting in San Antonio, was an exciting time for those who attended. As the local host society, we helped with meeting events and we had the

opportunity to view over 100 exhibits and many informative research presentations. Our TSM booth, decorated with a Texas theme, was visited by many, including several who joined the society. After the meeting, I contacted all the exhibitors, inviting them to join TSM. If you know of potential corporate members, please give me their contact information.

At our business meeting in San Antonio, we voted to name our student award the "Howard J. Arnott Student Presentation Award". We honor Howard's contributions to the society but particularly his many years of mentoring students and encouraging their participation in the Texas Society for Microscopy. Howard's students have given us insight into countless interesting and unusual topics. He is a roll model not only for students but he inspires his colleagues as well. An endowment fund also will be established and your contributions will help to ensure the future of this award.

The spring 2005 meeting will be a celebration of the 40th anniversary of the society. If you are interested in being involved in the planning of this notable meeting, please volunteer to help make this a memorable time. Pam Neill and I will be compiling a history of the society and we welcome your input. We particularly need help locating former members and hope to have many of our past presidents in attendance. As we celebrate the past, let us look toward the future with anticipation.

Ann E. Rushing
TSM President 2003-2004

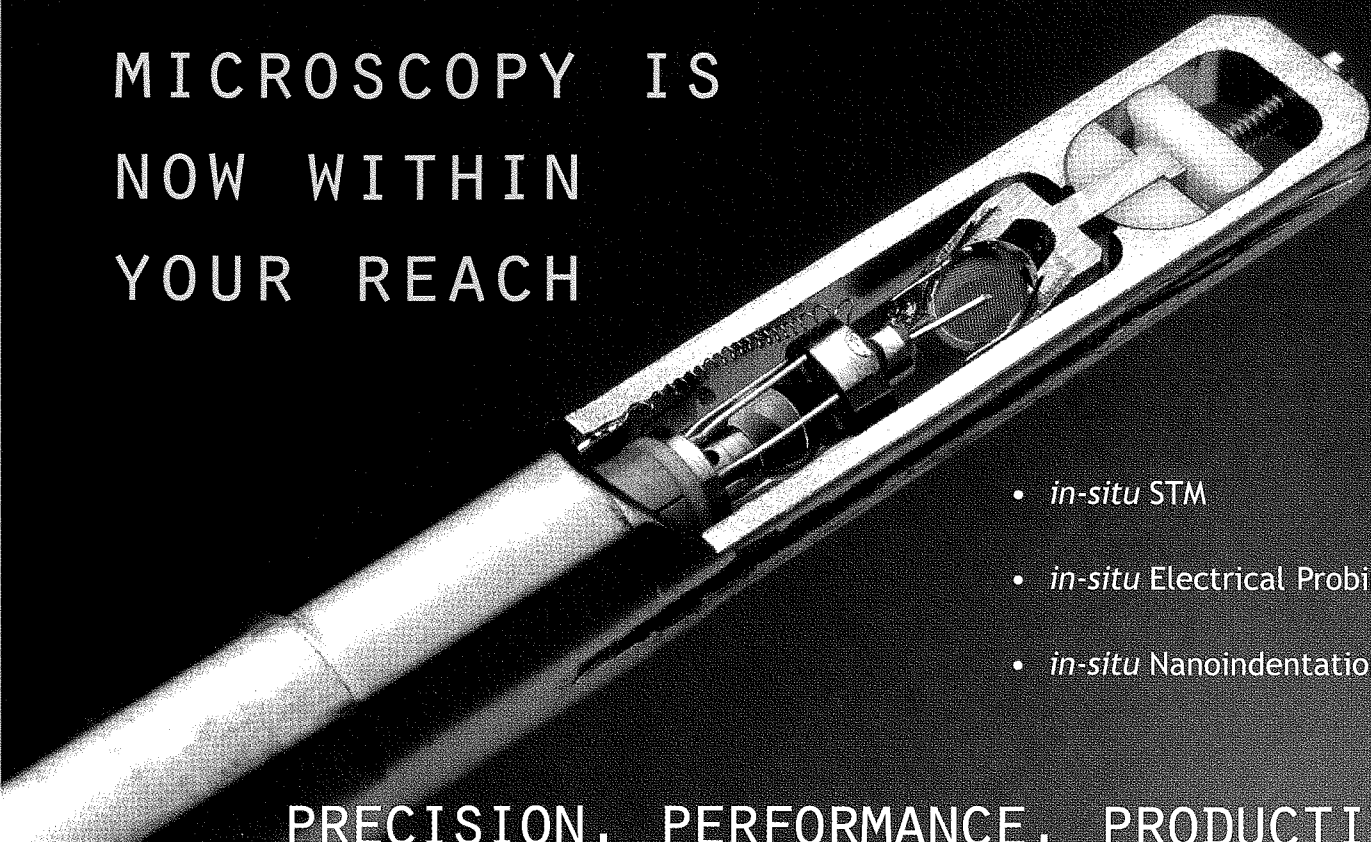
Call For Papers

Manuscripts are needed for the next edition of the Texas Journal of Microscopy. Please send your work as short communications, full articles or review articles in biological sciences, material sciences or education to:

Camelia G.-A. Maier
TSM Journal Editor
Department of Biology, TWU
Denton, Texas 76204-5799
(940) 898-2358
cmaier@twu.edu

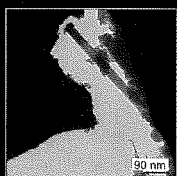
Manuscript deadline is July 15, 2004

IN-SITU PROBING MICROSCOPY IS NOW WITHIN YOUR REACH

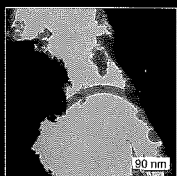


- *in-situ* STM
- *in-situ* Electrical Probing
- *in-situ* Nanoindentation

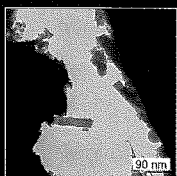
PRECISION. PERFORMANCE. PRODUCTIVITY.



In-situ Probing Microscopy within the small dimensions of a TEM specimen holder tip allows microscopists to combine the power of TEM and SPM at atomic resolution.



In-situ probing holders from Gatan* allow the nanocharacterisation and electromechanics of novel materials such as Nanotubes, Semiconductor Nano-structures, Nanowires, Nanoparticles, Field Emitters and Thin Films.



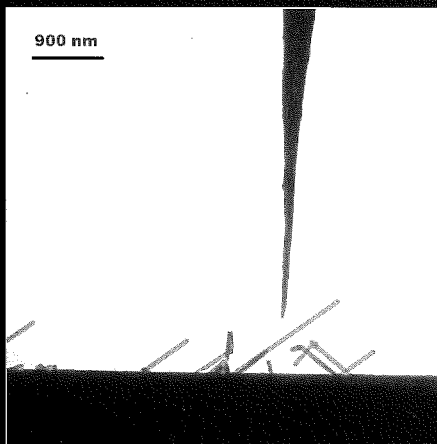
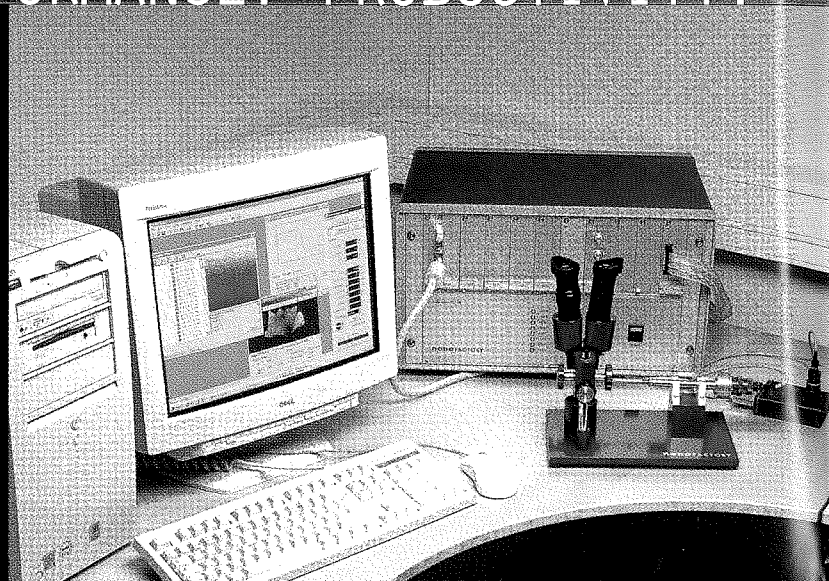
Incorporating miniaturised 3-D movements, achieved using a patented piezo micropositioning device, it is also possible to observe Electron Transport and Force Interactions.

Visit www.gatan.com/holders/nanofactory to view Examples of *In-situ* Probing Holder Applications.



Visit www.gatan.com/training for information on Gatan's newly-introduced "SPM-TEM Nanocharacterization Training School" taking place June of 2004.

www.gatan.com



Far Left-hand Images (from top to bottom): Gold tip probe moved close to a silicon nanowire under the electron beam of the TEM using a STM-Holder. TEM pictures courtesy of E. Olsson, K. Svensson and H. Olin, Chalmers University of Science and Technology.

Left-hand Image: Tungsten probe investigating the electrical properties of a semiconductor nanowhisker. TEM picture courtesy of Magnus Larsson, Reine Wallenberg, NCHREM, Lund University.

* Distributed by Gatan for Nanofactory Instruments AB, Sweden.

Treasurer's Report

Treasurer's Report 2004 Year End

Assets as of January 1, 2003:

Checking Account No. 005772227833 (Bank of America)	\$ 819.41
Certificate of Deposit No. 0940012289323 (Bank One)	4310.81
Total	\$ 5130.22

Income:

Spring Meeting	1350.00
Donations	775.00
Dues	1045.00
Corporate Sustaining Membership	2700.00
Journal Advertisements	
33:2	400.00
34:1	2250.00
Interest	
Checking account	3.92
CD	242.67
Total Income	\$ 8766.59

Expenses:

Spring Meeting	\$ 1663.35
M&M Meeting	339.15
Journal	
34:1	2656.04
Office Expenses	
Bond	144.59
President's Plaque	68.50
Web Fees	129.80
General Mailings	350.00
Monthly Bank Charges	76.00
Total Expenses	\$ 5427.43

Assets as of December 31, 2003:

Checking Account No. 005772227833 (Bank of America)	3915.90
Certificate of Deposit No. 0940012289323 (Bank One)	4553.48
Total	\$ 8469.38

Treasurer's Report For Period Beginning August 1, 2003 and ending March 12, 2004

Assets as of August 1, 2003:

Checking Account No. 005772227833 (Bank of America)	\$ 3331.16
Certificate of Deposit No. 0940012289323 (Bank One)	4418.15
Total	\$ 7749.31

Income:

Spring Meeting	
Donations	650.00
Dues	330.00
Corporate Sustaining Membership	3600.00
Interest	
Checking account	3.06
CD	135.53
Total Income	\$ 4718.39

Expenses:

M&M Meeting	339.15
Office Expenses	
Bond	144.59
Monthly Bank Charges	28.00
Total Expenses	\$ 511.74

Assets as of March 12, 2004:

Checking Account No. 005772227833 (Bank of America)	11955.66
Total	\$ 11955.96

Abstracts

BIOLOGICAL SCIENCES SPRING 2004

CHALLENGES IN PREPARATION OF WOODY SPECIMENS FOR MICROSCOPIC EXAMINATION. MARTHA GRACEY AND HOWARD J. ARNOTT. The Department of Biology and The Center for Electron Microscopy, The University of Texas at Arlington, Arlington, Texas 76019

To successfully prepare wood for examination by SEM, nontraditional techniques often need to be employed. Sectioning wood more often than not leaves a series of tool marks and/or ragged cell wall edges along the viewing surface of the wood. Careful sanding helps in making preparations to be viewed in the dissecting microscope, however, sanding fills in the tracheids with sawdust obliterating the desired SEM views. Good surfaces for viewing in the SEM require sectioning with blades. The sliding microtome is the most important tool in preparing sections that can be used for both light and scanning microscopy. However, good preparations can be made for SEM by using razor blades to cut the surface being studied. Handling the sections sometimes leaves "forceps" marks on the surface. These tool marks, in accordance with Murphy's Law, are often located in the most interesting or desirable area of the specimen. Imperfections in the blade used to make sections can also make tool marks, which, because of the mounting medium, are generally imperceptible in the light microscope, but ruin a SEM preparation. Direction of cut on the piece of wood can influence the outcome. The hardness of the wood can obviously affect sectioning and many methods are employed to soften the wood and leave the structure intact. Other current challenges include crystals that dull the blade and "hard" wood that results in blade "chatter". Wood has a natural tendency to curl when thinly sectioned and this creates a problem for both light and electron microscopy. A number of useful techniques were suggested by Alex Wiedenhoef of the National Wood Products Laboratory at Madison, Wisconsin to alleviate the curling problem. These involve distressing the lignin before drying and drying sections between two slides. Other techniques have evolved as we worked with different wood. *Quercus stellata* (post oak) required treatment with EDT (1,2 diaminoethene) for some period and then the use of steam softening during the sectioning process. Using the latter technique we have been able to examine an 1866 frost ring of the post oak.

AN SEM STUDY OF A BRISTLECONE PINE (*PINUS LONGAEVA*) FROST RING FROM 4710 B.C. HOWARD J. ARNOTT. The Department of Biology and The Center for Electron Microscopy, The University of Texas at Arlington, Arlington, Texas 76019

Frost rings have been reported from the stems of bristlecone pines (*Pinus longaeva*) by many investigators. For many years, Tom Harlan and other members of the Laboratory of Tree-Ring Research, University of Arizona, have been developing a bristlecone chronology which currently extends back almost eight thousand years. Harlan investigated a "remnant log," designated LTRR # 01-684, found on the North side of Campito Mountain in the White Mountains of California. Two samples were removed and cross-dated, the older piece dated to 5072 B.C. In a second slightly younger piece of the same stem he found a frost ring at 4710 B.C.

This is the oldest known frost ring of *P. longaeva* and it was examined by light and scanning microscopy at UTA. Sections of the wood were made using the sliding microtome, and were stained with safranin for LM. Those for SEM were mounted on stubs and sputter coated with gold-palladium. Annual ring 4710 B.C. is about 0.3 μm in thickness and is a late frost ring. The damage in the ring is relatively light consisting of collapsed tracheids in about the last five late wood cells in each tracheid file. The exact nature of the tracheid collapse is not clear, however, it is often possible to follow tracheid files from the undamaged portion of the frost ring into the early wood tracheid files of the next annual ring. As the rays and tracheid files extend outward from the middle of frost ring, they bend at an angle of about 35°. When they enter the next younger ring, they bend back about 35°, so that the rays and tracheid files continue to run "parallel" to those in previous rings but are offset by about 65 μm . Unlike the tracheids, the ray cells are not collapsed but are often expanded, sometimes by as much as double, and appear to be filled with resin. As viewed by SEM, and unlike the ray cells, only a few tracheids are filled with resin, and most have an open lumen. Circular bordered pits are seen in many files of tracheids in both the frost and other annual rings; however, bordered pits were not seen in the collapsed tracheids of the frost ring.

A STUDY OF THE 1866 FROST RING IN POST OAK (*QUERCUS STELLATA*). HOWARD J. ARNOTT. The Department of Biology and The Center for Electron Microscopy, The University of Texas at Arlington, Arlington, Texas 76019

Frost rings in post oaks (*Quercus stellata*) have been reported from a number of sites in Southern Plains region of Texas, Oklahoma, and Arkansas (Stahle, 1990). The stem specimen ECK8A used in this study was from central Texas. It was collected and cross-dated by Tom Harlan of the Laboratory for Tree-Ring Research at the University of Arizona, who found that the 1866 annual ring was a frost ring. The specimen was dark brown, ring porous wood with annual rings varying in color and with a tendency to split radially. The wood was very hard and sections were difficult to make even after softening with 1,2 diaminoethane and boiling water. However, after softening, acceptable sections were made using a sliding microtome or razor blades. Sections for LM were studied unstained or stained with safranin; sections for use in SEM were mounted on stubs and sputter coated with gold-palladium. Transverse sections show broad wood areas subdivided by wide multiseriate rays, which may have thirty or more files of cells and are 300 μm in tangential thickness. In between the rays are areas composed of parenchyma, fibers, tracheids, vessels and uniseriate rays characteristic of oaks. Vessels in normal rings are round in sectional profile and have a diameter ranging up to 350 μm ; tyloses are found in the lumen of all vessels. In contrast, the vessels seen in the frost ring are lunate in profile shape (collapsed) but like the vessels in normal rings the lunate vessels of the frost ring are also filled with tyloses. Distal to each of the lunate or collapsed vessels, a tissue not present in normal rings is found. This tissue named "frost generated procambium" (FGP) is apparently responsible for the regeneration of the normal structure as frost conditions subside. The FGP cells are angular to polygonal as seen in both transverse and radial section and of 20-40 μm in diameter. Their cell walls are almost as thick as those of the vessels but are generally lacking any internal contents. It appears that division of the FGP cells may be

involved in two processes: (1) by virtue of the pressure generated by the growth of these cells, the precursor "pro-vessels" are collapsed to form the lunate vessels characteristic of frost rings; (2) the FGP may regenerate the vascular cambium so that normal growth can continue.

BACTERIAL COLONIZATION OF RESIN ENCRUSTATIONS IN THE LEAVES OF *PINUS ARISTATA*. HOWARD J. ARNOTT. The Department of Biology and The Center for Electron Microscopy, The University of Texas at Arlington, Arlington, Texas 76019.

One of the characters used to distinguish *Pinus aristata* (The Eastern Bristlecone) from *P. longaeva* (The Western Bristlecone) is the presence of numerous resin encrustations on the leaves of the former. The white resin encrustations of *P. aristata* are in sharp contrast to the green color of the leaves. In some trees the foliage has so many resin droplets that it has been compared to the great plague of human "dandruff." On the contrary, the leaves of *P. longaeva* are almost completely free of these resin droplets and this distinction was important in Bailey's separation of the two species. The resin deposits in *P. aristata*, which may be several millimeters in length and width, are irregular in shape and the surface is marked by cracks and many small circular holes. While most of these deposits are solid some still have resin in a liquid form. Many of the holes appear to be formed by the evaporation of resin solvents. Other surface features appear to be broken "bubbles" on the resin surface. Leaf sections show "pores" that are connected to the resin deposits; whether stomata were in the pores could not be ascertained. On a few plants collected along the Gold Camp Road East of Victor, CO, I found what first looked like purple-black resin deposits. Closer observation showed that the purple color was caused by the presence of cyanobacteria, which colonized the resin droplets and the area close around them. These filamentous cyanobacteria are found on the surface as well as interior to the resin deposits and have many of the characteristics of *Nostoc*, including the presence of heterocysts. Light microscopic sections of the resin deposits show the filaments of the cyanobacteria penetrating the resin deposits. The cyanobacteria were easily cultivated simply by placing "infected" leaves in distilled water. While the *Nostoc*-like filaments dominate the cultured cells, some "double cells" and/or "packets of cells" with the characteristic structures of *Anacystis* were also seen. The ecological importance of the bacterial colonization is of interest. Likewise the possible utilization of the resin as a carbon source for the bacterial cells is worthy of attention.

IMAGE ANALYSIS TECHNIQUES USEFUL IN FROST RING STUDIES. HOWARD J. ARNOTT. The Department of Biology and The Center for Electron Microscopy, The University of Texas at Arlington, Arlington, Texas 76019

Some unique ways of studying microscopic images of frost rings have been developed by applying image analysis techniques. I will describe several of these techniques which combine the use of Photoshop and Image Pro Plus and present an opportunity for a deeper understanding of frost rings. Frost rings, common in conifers and many flowering plants, develop in either the Spring or Fall (early or late frost rings) as the weather changes rapidly from one that supports growth to sub-freezing temperatures. Characteristic frost rings have been described in pines, firs, oaks, etc. Almost always they involve damage or change to all or some of the components derived from cambial activity. One of the first techniques involves isolating the cells that show damage using Photoshop. The entire frost ring can be highlighted so as to show it in its relationship to prior and later annual rings. File tracing, using color lines traced on tracheid or ray files, make us better observe the relative changes in file direction that are involved in frost ring formation. File tracing can also clearly outline the role that ray

expansion plays in frost ring formation. Files from the damaged part of the frost ring can be "isolated" using Photoshop to separate one file from another, to separate the individual cells of a single file, or to compare a tracheid file with a ray file. Once separated, individual files or cells can be compared radially or tangentially across the frost ring thus providing insight into the processes involved in frost ring formation. The area, length, width, perimeter, etc. of individual cells can also be measured using Image Pro Plus; measurements can be compared either radially or tangentially. Using separation techniques on an area of frost damaged cells, allows the creation of an "exploded diagram". Such a diagram can show the relationship between all of the individual cells and give insight into the direction and pressures, which cause the frost ring damage to come about. Fast Fourier Transforms (FFT) can be made for frost rings and compared with those for normal annual rings. Individually "isolated" cells can also be studied by FFT allowing easy comparison of structural elements.

A THREE-DIMENSIONAL RECONSTRUCTION OF A NORMAL VERSUS AN ACTIVATED GOLGI APPARATUS OF *SCHERFFELIA DUBIA*. JEFFREY MIRANDA and JOANNE T. ELLZEY, University of Texas at El Paso, Department of Biological Sciences, El Paso, Texas 79902

After experimental flagellar amputation of the green alga *Scherffelia dubia* (Prasinophyceae), a new flagellum is regenerated. Flagellar regeneration was used to study the Golgi apparatus (GA) activity by comparing a normal and an activated GA during flagellar scale production. *Scherffelia* possesses scale-covered flagella and rigid cell walls consisting of scale-like subunits which are processed within the GA. In comparing images of a normal with an activated *Scherffelia* GA, we hypothesized that *Scherffelia*'s GA in the activated mode would exhibit ultrastructural changes. The null hypothesis was that no ultrastructural changes would be observed in the experimental GA compared to the control. Electron tomography was used to reconstruct 300 sections from the normal and the activated GA using the IMOD program developed at the University of Colorado at Boulder. The control *Scherffelia* did not undergo de-flagellation and was fixed by high pressure freezing (HPF). The active Golgi was fixed by HPF, 30 minutes after de-flagellation. Dual-axis tomography was utilized to produce high-resolution (~0.6 nm) 3D models of the GA. In addition to the development of the computer models, 3D resin prototypes are being constructed at the W. M. Keck Border Biomedical Manufacturing & Engineering Laboratory at the University of Texas at El Paso. The results of the two 3D models, normal versus activated GA supported the hypothesis that the activated mode has ultrastructural changes, compared to the control GA. The normal mode GA had 22 cisternae, while the activated mode Golgi had 20 cisternae. Fewer cisternae in the activated Golgi apparatus may be due to the maturation of cisternae. The control GA had dilated cisternae compared to the activated GA. Secretory vesicles were more numerous in the control GA compared to the GA from the de-flagellated algae. We concluded that more image comparisons are needed.

A MICROSCOPIC INVESTIGATION OF THE INTER-ACTION BETWEEN *PUCCINIA VIRGATA* AND FIVE VARIETIES OF INDIANGRASS (*SORGHASTRUM NUTANS*). JOHN D. MATULA and JOSEPHINE TAYLOR, Department of Biology, Stephen F. Austin State University, Nacogdoches, TX 75962.

Indiangrass (*Sorghastrum nutans* L. Nash) is a warm-season, perennial bunch grass used to revegetate and reclaim grasslands. The autoecious rust fungus *Puccinia virgata* is a common pathogen of indiangrass. A recent field evaluation by monitoring disease severity over time was able to categorize each of five indiangrass

varieties as either highly resistant, moderately resistant, moderately susceptible, or highly susceptible to this rust. A microscopic investigation was conducted to determine if the pathogen behavior at early stages of infection was affected by genotype, leading to the differences in susceptibility observed under field conditions. One-month old plants of five indiagrass varieties were artificially inoculated with rust uredospores. Germ tubes and appressoria were stained with 0.1% calcofluor and visualized under UV epillumination. Chi square analysis revealed that spore germination showed a slight dependence ($p=0.01$) on variety, whereas successful appressorium formation was very dependent ($p<0.0001$) on variety. Scanning electron microscopy was used to characterize the differences in leaf micromorphology between varieties. In addition, fungal colony length within leaf tissue of each variety was measured at 4 and 8 days post-inoculation to determine if post-penetration mechanisms were also contributing to the differential susceptibility observed.

HISTOMORPHOLOGICAL, HISTOCHEMICAL AND BIOCHEMICAL STUDIES ON THE PANCREAS AND DUODENUM IN PANCREATECTOMIZED AND ALLOXAN TREATED FOWL (GALLUS DOMESTICUS). DEB MAHAPATRA and NABARUN GHOSH, Department of Life, Earth and Environmental Sciences, West Texas A& M University, Canyon, TX 79016

Diabetes mellitus is a clinical condition caused either by the destruction of beta cells or insufficient production of insulin from the islets of Langerhans in case of the vertebrates. Interestingly however, in birds, unlike other mammals, experimental pancreatectomy or administration of the beta cytotoxic agent alloxan does not alter the homeostasis of blood glucose metabolism or show symptoms of diabetes. In our present investigation, two groups of birds were chosen. To one group alloxan was administered at the rate of 250-mg/kg body weight intravenously. To the other group pancreas were surgically removed. In both the groups, blood was collected at every 8-hour interval for biochemical estimation of serum glucose. Results in both the groups revealed an initial phase of hyperglycemia followed by normoglycemia and hypoglycemia. Histopathology through special staining revealed vacuolations, beta cell degeneration in the pancreatic islet and the presence of cell types in duodenum having characteristics similar to those of pancreatic islet cells. Our study reveals that duodenum might be used as the possible extra-pancreatic source for the beta and alpha cells.

DEVELOPMENT AND PERFORMANCE OF SILKWORMS (BOMBYX MORI) AS FUNCTION OF MULBERRY SEXUAL DIMORPHISM. CORINA MORARU¹, *REBECCA JOHNSON¹, DAVID C. GARRETT², HOWARD J. ARNOTT³, and CAMELIA G.-A. MAIER¹. ¹TWU, Department of Biology, Denton, Texas 76201, ²UNT, Department of Materials Science, Denton, Texas, 76201, and ³UT Arlington, The Department of Biology and The Center for Electron Microscopy, Arlington, Texas, 76019

Plants have evolved both constitutive and inducible strategies to defend themselves against herbivores, among those accumulation of mineral depositions and phytoestrogens. Previous studies in our laboratory showed that female leaves contain significantly higher levels of oxalate and calcium depositions, and showed significantly higher estrogenic activity than male leaves of mulberry, *Morus alba*, *Moraceae*, the only natural food for silkworms, *Bombyx mori*. We used the mulberry/silkworm system, a specialist insect herbivore system, to investigate the impact of the above characteristics of mulberry sexual dimorphism on larval feeding and development. Length and weight of individual caterpillars were estimated in two populations of silkworms, one fed exclusively with male mulberry leaves, the other one fed exclusively with female leaves, and feeding behavior on male and female leaves was observed. Silkworm

feeding on male leaves was significantly greater than on female leaves. Not only that they performed better on male than female leaves, but also they preferred male to female leaves. Total time of feeding on male leaves was twice as long as that of feeding on female leaves. Development was delayed for silkworms raised exclusively on female leaves. Although both male and female mulberry leaves contain same types of mineral depositions, calcium carbonate lithocysts, and calcium oxalate druses and prismatic crystals, at the same anatomical location, insoluble oxalate concentrations and calcium carbonate deposits were significantly higher in female than male leaves ($P=0.033$ and $P=0.02$ respectively, $\alpha=0.05$). In free feeding experiments, silkworms avoided chewing on female leaf veins, which contained significantly higher concentrations of calcium oxalate deposits than the male veins. Extracts of female-fed silkworm feces induced lower estrogenic activities than the male-fed ones suggesting better assimilation by silkworms of phytoestrogens in fresh female leaves. Silkworms prefer and performed better on male mulberry leaves possibly due to their low content of mineral depositions, oxalate, and phytoestrogen activity.

MICROSCOPIC STUDIES OF TRAPS AND SEEDS OF CARNIVOROUS PLANTS. LEA C. SAVOLAINEN and CAMELIA G.-A. MAIER*. Department of Biology, Texas Woman's University, Denton, TX 76201

Certain plant species known as carnivorous plants have evolved organs to capture and digest animal tissues in order to obtain the nutrients they need, especially nitrogen. Carnivorous plant species are flowering plants, which live in acidic, nutrient-deficient soils. They use various techniques, such as hair-triggered traps, pit fall traps, sticky leaves, etc. to capture mostly insect prey. The traps of *Dionaea muscipula* and *Nepenthes fuscata* (Sarawak) were dissected and fixed for electron microscopy, to study the mechanisms responsible for the capture of prey. In addition, we report for the first time on the morphology of seed coats and seed germination, very important traits in the phylogeny and identification of carnivorous plant species. Dry and germinated seeds from four genera and nine species were prepared and studied under light and scanning electron microscopy.

PERIDERM DEVELOPMENT IN ULMUS CRASSIFOLIA NUTT. ANN E. RUSHING and SONJA M. SKROVANEK. Department of Biology, Baylor University, Waco, TX 76798.

Periderm is produced as a protective layer in most dicotyledonous plants that increase in diameter during development. Cedar elm, *Ulmus crassifolia*, produces a circumfluent periderm and subsequently initiates winged cork by uneven development of localized regions of these peridermal layers. Scanning electron microscopy reveals that cedar elm first produces a uniform and circumfluent periderm comprised of 5-6 layers of cork cells. Radial expansion of portions of these existing cork cells initiates wing formation, with the resulting protrusion often rupturing the original epidermis. After initial radial expansion of existing cells, new layers are added to the wing by increased cell divisions in the phellogen (cork cambium), followed by radial expansion of the newly produced cells. Wings are oriented laterally on opposite sides of the stem, although one wing typically develops well before the other is visible. During early stages of wing formation, the cork cambium in the remainder of the stem does not appear to be active. A similar type of wing development also has been reported in *Acer*, *Quercus*, *Liquidambar*, and other species of *Ulmus*. In contrast, wings in *Euonymus alatus* are formed by localized growth of the cork cambium prior to full periderm initiation.

THE EFFECTS OF ESTRADIOL BENZOATE ON THE THINNING OF ZEBRA FINCH EGGSHELLS. HODA EMAM, HAIFA JAMALEDDINE, CYNTHIA LUNA, KINJAL SHAH, SANDY WOEHRLE and SANDRA WESTMORELAND. The Department of Biology and the Center for Electron Microscopy, University of Texas at Arlington, Arlington, Texas 76019

Researchers have found that birds exposed to foreign estrogens show reproductive failure, growth retardation, life-threatening deformities, and alterations in their brains and liver function. Increased egg breakage due to the thinning of the eggshells has been shown as a major consequence of exposure to oral estrogen. The purpose of the current study was to determine if estradiol benzoate has an effect on shell thickness. Our hypothesis was that exposure to oral estrogen causes the eggshell to become significantly thinner. Zebra finch birds were orally administered estradiol benzoate or canola oil (for controls) once daily by Jim Milliam at the University of California at Davis. Eight eggshells from the zebra finch birds were shipped to the University of Texas in Arlington for analysis (four control and four experimental). The eggshells were cleaned in distilled water and air dried. Samples were taken from the equator region (the largest diameter of the egg) and then mounted with carbon paint on stubs. The shells were then coated with gold and palladium and viewed with scanning electron microscope. Digital micrographs were made of shell samples and shell measurements were made using Vital Scan computer program. The birds treated with estradiol benzoate produced eggshells that were significantly thinner than the control eggshells. We found that in the experimental eggs the mammillary cones were reduced in size and were not as distinct as in the control eggs. This may have contributed to measuring errors. Because shell thickness varied from egg to egg, this experiment should be repeated with a greater number of eggs.

ELECTRON MICROSCOPY ANALYSIS OF GENTOO PENGUIN EGGSHELLS. SHADAB RAHMANI, SANDRA L. WESTMORELAND. The Department of Biology and The Center for Electron Microscopy, University of Texas at Arlington, Arlington, Texas 76019.

The avian eggshell provides calcium for the embryo during the time of incubation. In fertile eggs the vascular chorioallantoic membrane transfers calcium from the shell internally to the chick. In the current study three different Gentoo penguin eggs were provided by Newport Aquarium for analysis due to hatching problems. Egg 1 was an artificially incubated egg; it was fertile but it did not hatch. Egg 2 was naturally incubated, but it was not fertile. Egg 3 was 90% naturally incubated and 10% artificially incubated; it was fertile and it successfully hatched. Three hypotheses were proposed. Shell structure of all penguin eggs would be consistent with avian shells previously studied. No calcium loss was predicted in the airspace region of any eggs because the shell membrane and the chorioallantois are separated from the shell so no calcium can be removed. Evidence of calcium removal would be seen in the equator region of the shells of fertile, incubated eggs (eggs 1 and 3). Samples were broken from the shell in two regions of each egg, the air space and the equator region. Three pieces of shell from each region of the eggs were mounted and taped on aluminum stubs

and coated with gold. Two different sets of stubs were prepared. The first six stubs were untreated, but the second set was treated with 5% sodium hypochlorite for 90 minutes to remove the membrane. The stubs were viewed on a scanning electron microscope. In none of the eggs was calcium loss seen in the airspace region. In the fertile eggs (1 & 3) calcium loss was seen in the equator region. In the non-fertile egg (2) no calcium loss was seen in the equator region. These results concurred with our hypotheses. We viewed unusual structures in the inner shell region. The penguin eggshells have a different shell structure than other avian eggshells previously studied. Shortened structures were present between the mammillary cones. Whether these are abnormalities or a primitive shell feature requires further study.

CHANGES IN EGGSHELL OF JAPANESE QUAIL DURING EMBRYOGENESIS. SANDRA WESTMORELAND*, TINA HALUPNIK*, and PATRICIA HESTER**. *The University of Texas at Arlington, Department of Biology, Arlington, Texas 76019; **Purdue University, Department of Animal Science, Lafayette, IN 47906

The avian eggshell is a source of calcium for the developing embryo. Movement of calcium from the shell to the embryo occurs once the chorioallantois is in place and functional. At the blunt end of the egg the chorioallantois has no contact with the shell due to the airspace and no calcium loss occurs. The purpose of the current study was to investigate changes that occur in shells of fertile Japanese quail eggs during incubation in order to have a baseline study for comparison to eggs that were incubated at the MIR space station. It was hypothesized that when eggs reached the stage at which the chorioallantois was in place, shell samples from the equator region (largest shell diameter) would show signs of calcium loss and reduced shell thickness, while samples from the airspace would not. Fertile Japanese quail eggs were collected from a breeding colony at Purdue University. Incubation of the eggs was interrupted at six different intervals: 3, 7, 10, 12, 14, and 16 days. Eggshells were shipped to The Center for Electron Microscopy at The University of Texas at Arlington for analysis. Shells of three eggs for each incubation date were sampled in two regions, the airspace and equator. From each region five radial samples and one inner shell surface sample were prepared for viewing on the scanning electron microscope. Digital micrographs were taken to document shell changes. Measurements were collected of shell thickness for each radial sample. No changes were observed in shell samples from either airspace or equator in eggs incubated 12 days or less. In eggs incubated 14 or 16 days voids were seen in the mammillary cones of equator samples; no voids were found in airspace samples. For any given day of incubation, the equator region shell samples were consistently and significantly thicker than airspace samples. In eggs that had been incubated 14 and 16 days, the equator samples approached the thickness of the airspace samples. This trend is interpreted to indicate that shells are normally thicker at the equator than the airspace region, but the relative shell thickness changes at day 14 of incubation when the equator region becomes thinner due to calcium loss.

CALLUS DEVELOPMENT AND SOMATIC EMBRYOGENESIS IN DIVERSE EXPLANTS OF COWPEA, *VIGNA UNGUICULATA* (L.) WALP. GEORGE OMWENGA and DON W. SMITH, Department of Biological Sciences, University of North Texas, Denton, Texas 76201

Five cowpea, *Vigna unguiculata* (L.) Walp., genotypes; UCR 519, UCR 694, UCR 696, UCR 779 and Petite-N-Green (PNG) were evaluated for callus development and somatic embryo formation.

Explants were obtained from primary leaves, hypocotyl and cotyledon and were cultured on Murashige and Skoog (MS) medium supplemented with 1.0, 3.0 and 6.0 mg/l dicamba or picloram. After one month of culture 60-100% explants produced calli but no shoots. Culture of calli raised on MS medium supplemented with 3.0 mg/l dicamba or picloram in liquid culture resulted in production of cotyledonary stage embryos that did not germinate.

FLUORESCENT MICROSCOPY ON THE BSBMV (BEET SOIL BORNE MOSAIC VIRUS) INFECTED SUGAR BEET (*BETA VULGARIS*) FOLIAGE

NABARUN GHOSH, MARIA E. VILLANUEVA, and DEB MAHAPATRA
Department of Life, Earth and Environmental Sciences
West Texas A& M University, Canyon, TX 79016

Sugar beets (*Beta vulgaris* L.) represent a major segment of the sweetener industry in the United States. Beet soilborne mosaic virus (BSBMV) is a member of the genus Benyvirus that infects sugar beets (*Beta vulgaris*). Rhizomania, caused by BNYVV (Beta Necrotic Yellow Vein Virus) is a type member of the genus Benyvirus, vectored by a fungus *Polymyxa betae*, and BSBMV is one of the most devastating disease of sugar beet in the United States, responsible for the vast decline of crop production in the last decade. The Southwest region, and the Great Plains have experienced a decline in sugar beet production in the last 10 years (1). Although the rhizomania diseases have been widely investigated for many years, BSBMV was identified for the first time in Texas in 1988 (2). Extensive research is needed to localize and control these pathogens. Rhizosphere soil from sugar beet with foliar symptoms of BSBMV and BNYVV were collected from sugar beets fields from Colorado, Nebraska, Minnesota and Texas. Soil samples were bioassayed. Systemically infected sugar beet leaves (Fig. 1) were harvested from the bioassayed samples. Infection was confirmed by a modified double antibody sandwich enzyme-linked immunosorbent assay (DAS)-ELISA as describe by Heidel (2). To study the leaves and petioles with epifluorescence, fairly thin, but not super thin sections were cut from the beet leaves and petioles using double-edged sharp razor blades. The sections were stored in labeled vials containing 75-80% glycerin. Each set

of sections were observed and images were captured using a BX-61 Olympus microscope attached to a Magnifire Digital Camera and a UV source. The untreated sets were examined for autofluorescence. The other sets were treated with berberine hemisulfate and counterstained with aniline blue. Another set was stained in fluoro yellow for possible localization of the suberin components especially in the cork tissue. UV radiation was used as the source, whereas blue light helped in fluorescing the lignified tissue very well. We observed the sections from the leaves and petioles at different magnifications for possible localization of viral elements. Autofluorescence was recorded in the epidermis and hypodermis region of the petiole (Fig. 2). Sugar beet leaves emit BGF (Blue-green fluorescence) that results in autofluorescence (3). Variation of fluorescence was recorded between the infected and non-infected regions while using the FITC filters (Figures 4, 5, 6). It has been reported that structural changes due to the mechanical damages of the beet leaf tissue could result in epifluorescences (4). The presence of several inclusion bodies was observed in the infected tissues. There are previous reports of such inclusion bodies in infected tissues of turnip, tobacco and potato and even a classification of virus-induced inclusions (5). The future objective of this study is to confirm the localization of beet viruses in other organs using different techniques.

References

1. Rush C.M. and Heidel G.B. 1995. Furovirus disease of sugar beets in the US. Plant Disease 79: 868-75.
2. Heidel G.B., Rush C.M., Kendall T.L., Lommel S.A., and French R. C. 1997. Characteristics of beet soilborne mosaic virus, a furo-like virus that infects sugar beets. Plant Disease 81: 1070-1076.
3. Morales F., Cerovic Z., and Moya I. 1996. Time resolved blue-green fluorescence of sugar beet (*Beta vulgaris* L.) leaves. Biochemica et Biophysica Acta 1273: 251-262.
4. Ibrahim L., Spackman V. M. T., and Cobb A. H. 2001. An investigation of wound healing in sugar beet roots using light and fluorescence microscopy. Annals of Botany 88: 313-320.
5. Edwardson J.R. and Christie R. G. 1978. Use of virus-induced inclusions in classification and diagnosis. Ann. Rev. Phytopathol. 16: 31-55

Epifluorescence on BSBMV-infected sugar beet tissues.

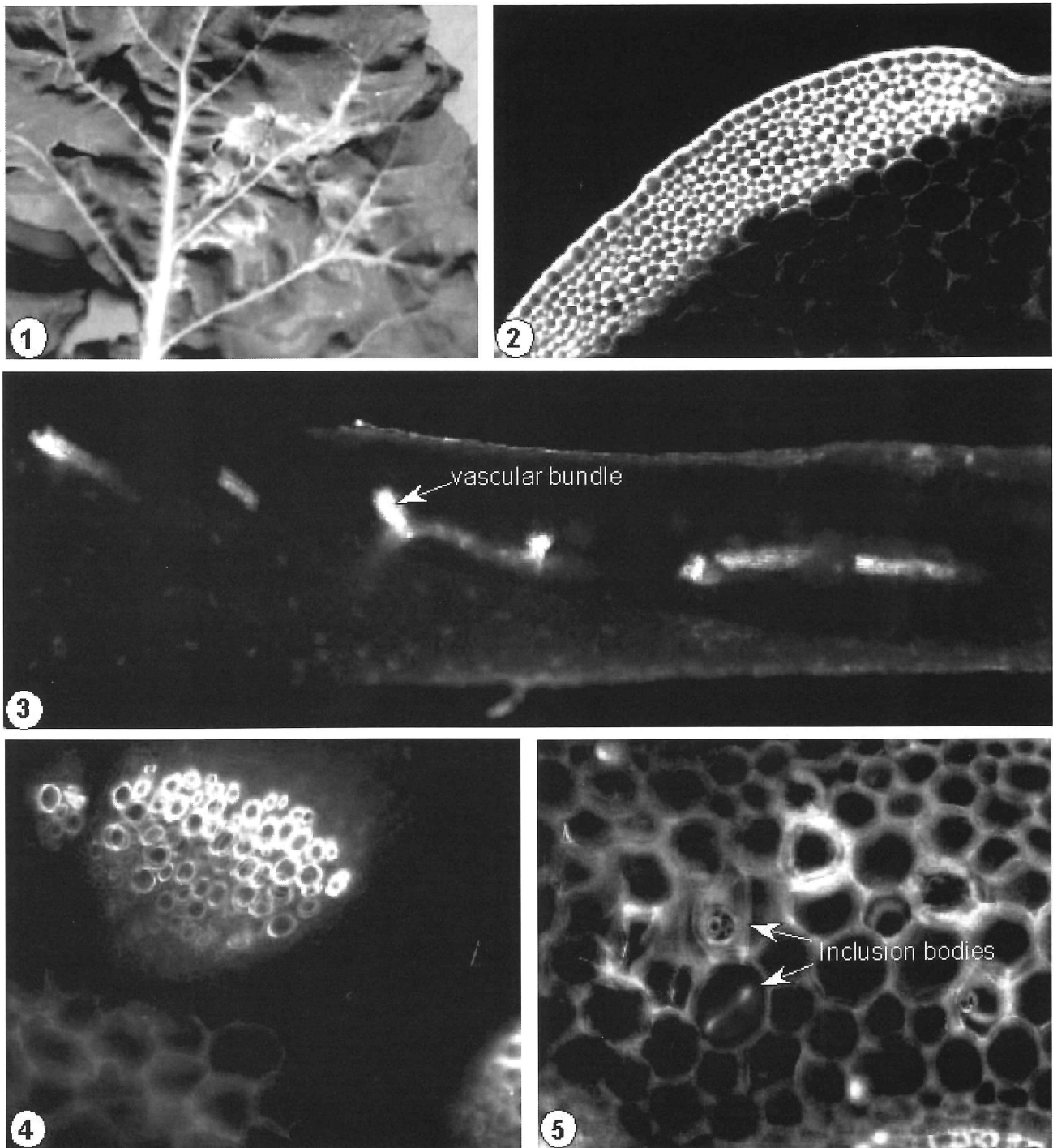


Fig. 1 - Morphology of an infected leaf from a systemically-infected beet plant. Fig. 2 - Autofluorescence in the epidermis and the hypodermis of petiole. Fig. 3 - Fluorescence in the vascular bundle in the transverse section of an infected leaf stained with fluolol yellow. Fig. 4 - Vascular bundle of an infected petiole. Fig. 5 - Infected leaf tissue showing inclusion bodies (arrows).

COMMON FAILURE MODES IN SN/PB SOLDER JOINTS

JODI A. ROEPSCH

Raytheon Network Centric Systems, McKinney, TX 75071

Solder joints can potentially fail by several different means depending on the condition of the joints as well as stresses applied to these joints. Solder joint failures are common and many conditions may contribute to such a failure. For example, a joint may fail due to excessive intermetallic growth, gold embrittlement, excessive voiding, low solder volume or CTE mismatch in combination with an applied stress such as thermal fatigue, shear stress, tensile stress, and vibration. Solder joint reliability can have high risks associated with failure. For example, aerospace and military applications can result in a life or death situation if a system should fail.

Intermetallic growth is a time temperature dependent occurrence. Tin/Lead (Sn/Pb) solder is commonly applied to nickel (Ni) or copper (Cu) surfaces. In order for a good solder joint to be present, an intermetallic must form. It can be a problem when excessive intermetallics form since the intermetallics are more brittle than the solder and therefore are more prone to fracture. If too much stress is applied to such a joint, the joint could fracture through the intermetallic leading to failure. Figure 1 is an example of a failure when shear stress is applied to a joint resulting in fracture through the intermetallic layer.

Gold embrittlement is a specific type of failure due to intermetallic formation. Many surfaces to be soldered contain a protective gold (Au) plating layer. The purpose of such a layer is to protect the surface to be soldered from oxidation to prevent de-wetting or non-wetting of the solder. Upon soldering, the gold layer

is absorbed by the solder allowing the solder to then wet to the underlying surface. If the gold layer is too thick in comparison to the solder volume used for the joint, then excessive Au/Sn intermetallics may form leading to gold embrittlement. In general, 5 wt% or less gold in a solder joint should not lead to embrittlement.¹ Above this amount, a brittle zone may form in the joint subsequently leading to fracture. Figure 2 is an example of excessive Au/Sn intermetallic formation.

Coefficient of Thermal Expansion (CTE) characteristics of materials surrounding a solder joint are important in the reliability of the joint. A mismatch of materials could be detrimental to the solder joint. For instance, device material or coatings on a PCB (Printed Circuit Board) may have significantly different CTE values than the board material. Thermal excursions can cause movement of the device, stressing the solder joints.

Excessive voiding within a solder joint as well as a low solder volume can result in failure due to decreased joint strength. In many applications, a certain amount of voiding is acceptable. Voiding can result from a lack of solder volume, outgassing of a contaminant, or a lack of solder wetting to a surface.

The amount of stress applied to a joint is key to the reliability of the joint. When in excess, failure may occur. For example, shear and tensile stress, thermal stress, mechanical shock, as well as vibration are known to lead to fractured solder joints. In many cases, it is a combination of the condition of the solder joint and the stress applied to the joint that results in solder joint failure.

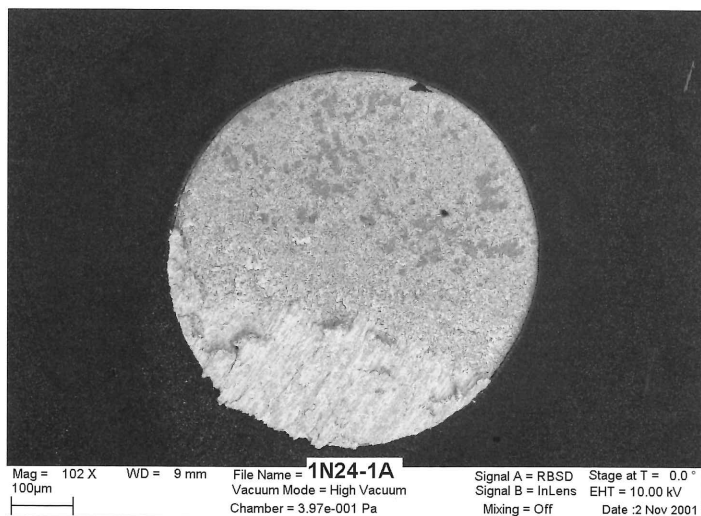


Figure 1: SEM image of failed solder joint due to excessive shear stress. Lateral cup and cone is present in the remaining solder viewed in the lower portion of the pad. The fracture occurred through the intermetallics along the upper two thirds of the pad.

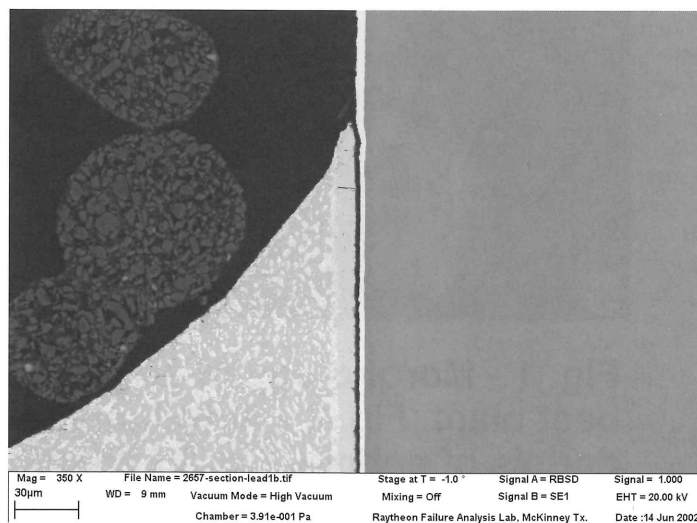


Figure 2: The crack is extending through a brittle zone due to excessive Au/Sn intermetallics.

(Endnotes)

¹ Daebler, D., "An Overview of Gold Intermetallics in Solder Joints", Surface Mount Technology, October 1991, pp. 43-46.

ADVANCED PROCESSING OF SPECTRAL IMAGING DATA SETS. PATRICK P. CAMUS, Thermo Electron, 5225 Verona Road, Madison, WI 53711

Traditional EDS analyses consist of spectra from points, and line-scans and maps of pre-selected elements. Very little post-processing or analysis of the non-spectral data is possible. The advent of spectral imaging acquisition changes that ability. Spectral imaging EDS acquisitions collect a complete spectrum at each point in an image scan. This data is then able to be analyzed as often as necessary while changing as many parameters as necessary to fully understand the material under investigation.

It is well known that peak counts in spectra are not directly related to the material chemistry. It is necessary to include absorption and peak deconvolution to accurately report the composition. In the same manner, simple elemental count maps do not provide a good indication of the composition of the material. Quantitative mapping needs to be performed which takes into account spectrum background, absorption, and peak deconvolution. Since spectral imaging stores all of the x-ray data, the quantitative analyses can be performed at any later time with any set of elements with any additional correction options.

As useful as quantitative mapping results are, they do not provide a summary description of the compound distribution in the material. The analyst is usually interested in the number and distribution of distinct and unique chemical compounds in the material, not necessarily the element distributions. Multivariate statistical analysis of the complete spectral imaging data set provides results for each unique component in the material. In this way, the very large spectral imaging data set can be reduced to a manageable and complete description of the sample. Examples of quantitative mapping and multivariate statistical analyses of spectral imaging data sets collected in the SEM and TEM will be presented.

**TECHNICAL
SPRING 2004**

XPLORE 3D: A TOTAL SOLUTION PACKAGE FOR ELECTRON TOMOGRAPHY. LINDA MELANSON, FEI Company, Hillsboro, OR

Electron tomography has emerged as an important methodology for studying the three-dimensional structure of whole cells, cellular organelles and sub-cellular assemblies. This method involves collecting a series of images at increasing tilt angles and merging these data to reconstruct the three-dimensional volume of the specimen under observation. The past ten years have shown significant advancements in instrumentation in the form of computer controlled specimen stages, high sensitivity large format CCD detectors, stable Schottky field emission electron sources and energy filters. In addition, improvements in computational power and image processing techniques have made automated tomographic data collection and reconstruction possible. There are several tomographic acquisition, reconstruction and visualization programs currently available to the academic community. Xplore3D is an example of a complete software solution offered by FEI Company that provides a fast, reliable, automated means for acquiring, reconstructing and visualizing a specimen three dimensions (Fig. 1).

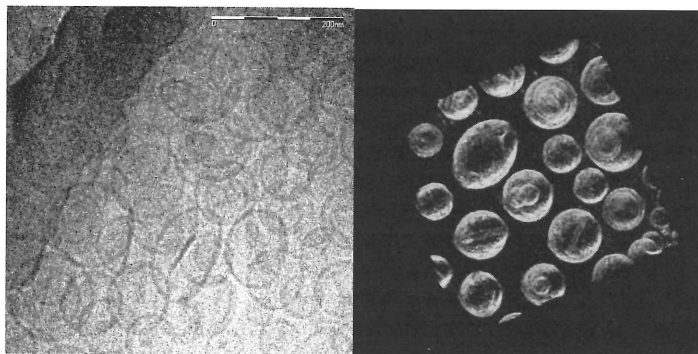


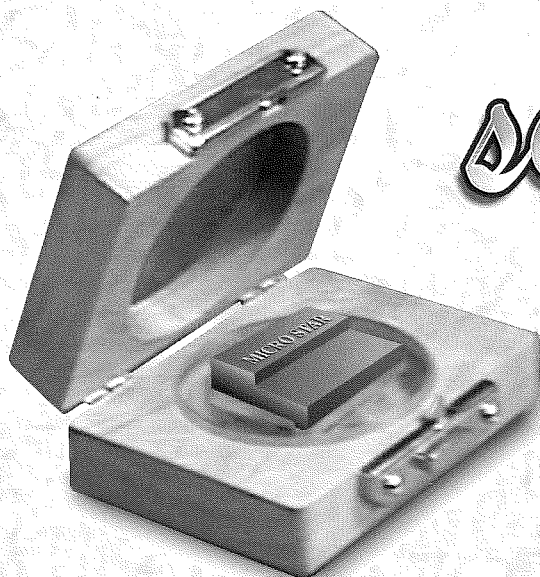
Figure 1. Drug loaded liposomes – Image is Cryo-EM (15K) tomography of doxorubicin-loaded vesicles recorded on a Tecnai Polara. Tomogram acquired at 2-degree increments through $\pm 50^\circ$ at a magnification 40,000 and a total dose $140 \text{ e}/\text{\AA}^2$. Images are courtesy of Dr. Peter Fredrik, EM Unit, University of Maastricht, The Netherlands.

ADVERTISER'S INDEX

Advertiser	Page Located	Advertiser	Page Located
Diatome U.S.	29	Micro Star Technologies, Inc.	2 & 18
Electron Microscopy Sciences	5 & 32	Soft Imaging Systems	20
Gatan	8	Ted Pella	4 & 28
M.E. Taylor Engineering, Inc.	31		

Quality

second to none.



Micro Star diamond knives superb quality is backed by an unprecedented 1 year guarantee. Micro Star, the leader in diamond knife technology is the choice of thousands of scientists around the world. See the reasons:

DIAMOND KNIFE BRAND	KNIFE TYPES	BOAT STYLES	ULTRAMICROTOMY KNIFE SIZES (mm)	KNIFE SIZES ABOVE 6mm	RESHARPENING FOR ALL BRANDS	SAFE NO TOUCH CLEAN SYSTEM	ONE YEAR GUARANTEE	RESHARPENING 3mm	3mm NEW KNIFE PRICE
"D1"	6	4	1.5 to 4	NONE	NO	NO	NO	NO	\$ 1,650
"D2"	6	5	1 to 5.5	NONE	NO	NO	NO	NO	\$ 1,700
"D3"	1	1	2 & 3 only	NONE	NO	NO	NO	NO	\$ 1,750
MICRO STAR	7	8	1 to 6	7 to 10	YES	YES	YES	YES	\$1,090
									\$1,990

Why pay more?

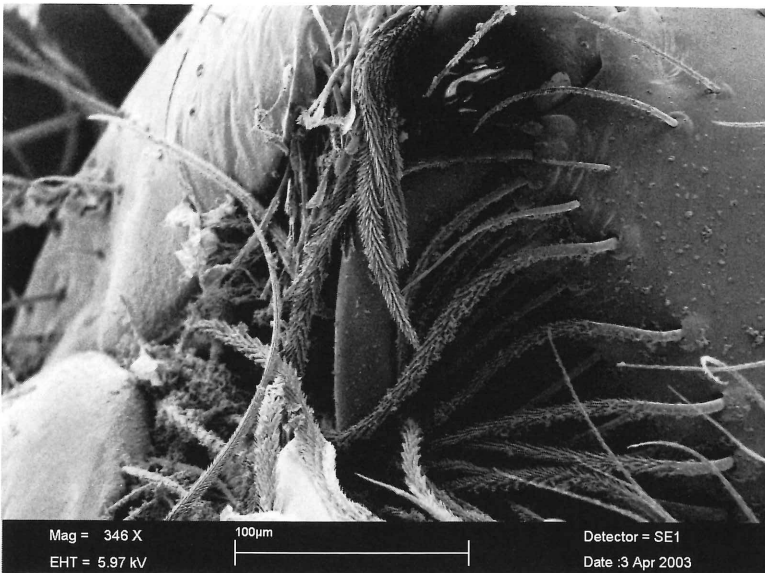
MICRO STAR DIAMOND KNIVES

800 533 2509 Fax 409 294 9861 e-mail: mistar@msn.com

Complete price list, specifications, dimensions and manual at our Web site:

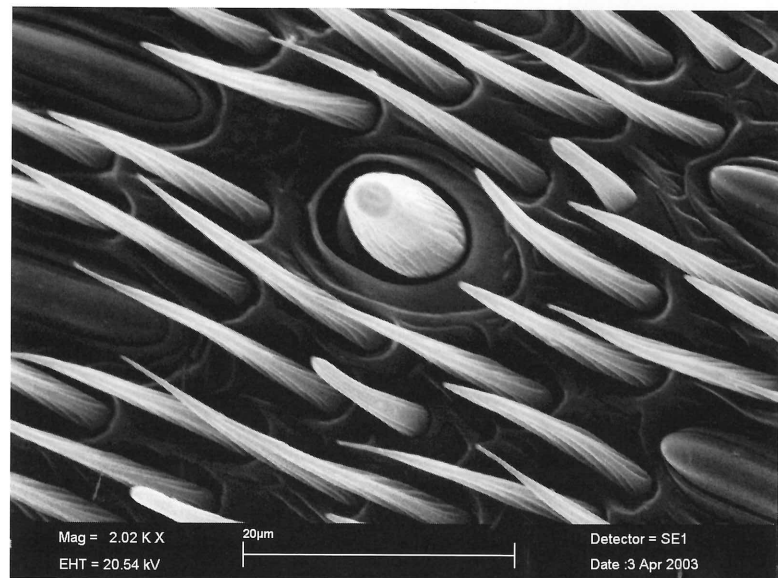
<http://www.microstartech.com/>

OUR STUDENTS



SEM of spider mouthpieces, photographed by **Chakavak Sara Farhangi**, **Dr. Anxiu Kuang's** student at The University of Texas Pan-American in Edinburg, Texas.

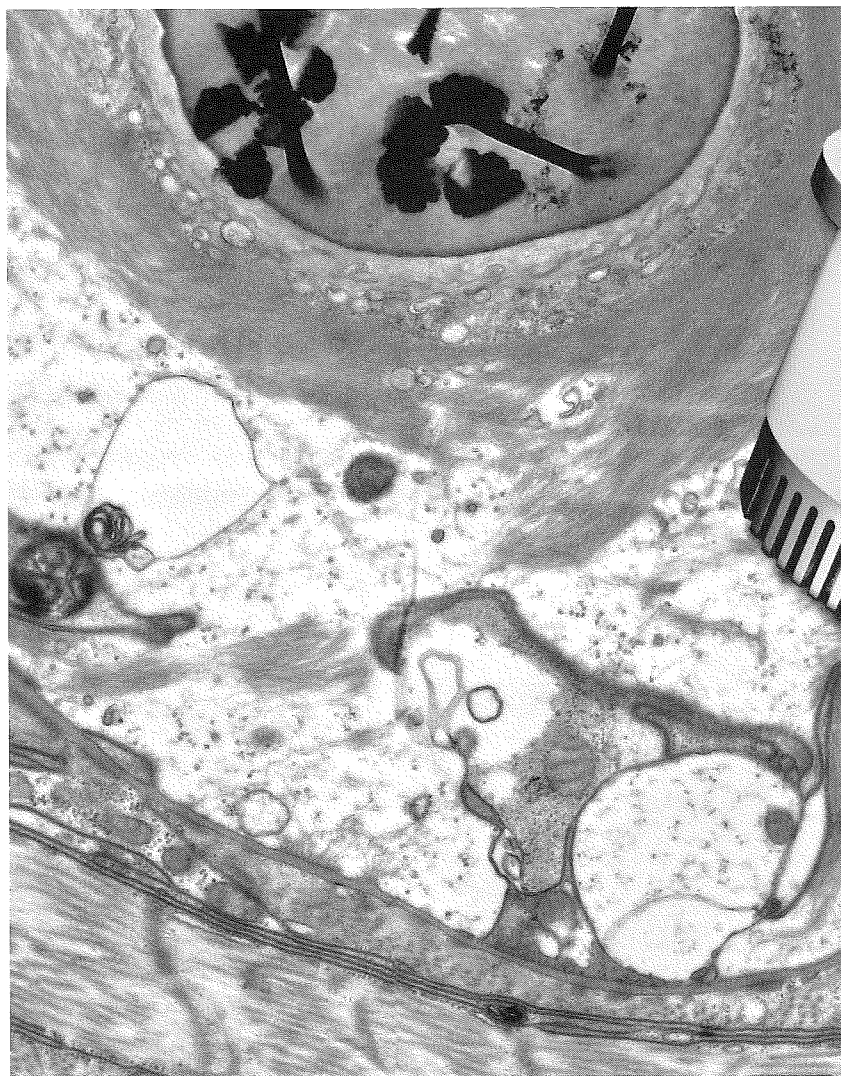
This SEM of the yellow jacket's antenna shows hairlike projections that are used as sensors and a peglike chemoreceptor. The sample was viewed using a LEO 435 VP SEM by **Maria Yanez**, **Dr. Anxiu Kuang's** student at The University of Texas pan-American in Edinburg, Texas.



SEM of open stomata. The guard cells are elliptic or kidney-shaped. Guard cells function as a hydraulically operated valve. Photographed by **Chakavak Sara Farhangi** at The University of Texas Pan-American.

KeenView

Fast - High Resolution - 12-bit CCD Camera



- Bottom Mount
- Resolution: 1376 x 1032 pixels
- Binning: 2x, 4x, 8x
- Dynamic range: 12-bit
- Chip Temperature: 10° C
- Peltier-cooled

Soft Imaging System offers high resolution, high sensitivity, easy to install cameras for Transmission Electron Microscopes, and Light Microscopes. A digital beam interface is offered for Scanning Electron Microscopes. All of our hardware systems integrate with analySIS® software - an image analytical system that provides you with microscope control, camera operation, optimized image acquisition, manual or automated image analysis, database archiving, report generation and more.

Digital Solutions for Imaging and Microscopy
Soft Imaging System



For detailed information please contact:

Soft Imaging System
info@soft-imaging.com
www.soft-imaging.com

North America
Europe
Asia / Pacific

(888) FIND SIS
(303) 234-9270
+ 49 (251) 79800-0
+ 60 (3) 8313-1400

CORPORATE MEMBERS



Allied High Tech Products, Inc.

2376 East Pacifica Place
Rancho Dominguez, CA 90220
(800) 675-1118 FAX (310) 762-6808
Robert Hocher
13409-B Saddlebrook Tr.
Austin, TX 78729
(800) 675-1118 ext 265
rwhochoer@alliedhightech.com

Atomic Spectroscopy Instruments, Inc.

Graham R. Bird
1021 Yellow Rose Drive
Salado, TX 76571-1035
(254) 947-8929
grbird@thegateway.net

Barry Scientific, Inc., Margrit Barry

P.O. Box 173, Fiskdale, MA 01518
(800) 348-2257 FAX (508) 347-8280

Biocare Medical, LLC.

Joel Martinez
2940 Camino Diablo, Suite 300
Walnut Creek, CA 94597
(800) 799-9499
jmartinez@earthlink.net

Beockeler/RMC

Dave Roberts
4650 S. Butterfield Drive
Tucson, AZ 85714
(520) 745-0001 or (800) 552-2262 FAX
(520) 745-0004
dave@boeckeler.com
www.rmcprouducts.com

Denton Vacuum, Inc.

John Crow/Graham R. Bird
Electron Microscopy & Research
Systems
1259 N. Church Street
Moorestown NJ 08057
(856) 439-9100 FAX (856) 439-9111

Digital Instruments – Veeco

Stephen Zeigler
4907 Finley Dr.
Austin, TX 78731
(512) 420-8147
zig_s@ix.netcom.com

EDAX, Inc., Gene Griggs

8021 North FM 620, Apt. 223
Austin, TX 78726
(512) 249-2418 FAX (512) 249-0548.
ggriggs@edax.com

Electron Microscopy Sciences/Diatome

Richard Rebert/Stacie Kirsch
321 Morris Road, P.O. Box 251
Fort Washington, PA 19034
(800) 523-5874 FAX (215) 646-8931
sgkeck@aol.com

Emispec Systems, Inc.

Michael Mizell
2050 South Cottonwood Dr.
Tempe, AZ 85282
(480) 894-6443 ext 28
FAX (480) 894-6458

Energy-Micro-Analytical Consultants

Walter J. Protheroe Jr.
8711 Beau Monde
Houston, TX 77099-1107
(713) 879-7211

FEI Company

Jo L. Long 1902 Pepper Hill Way
Houston, TX 77058
(281) 480-4015 FAX (281) 480-2708
jlong@feico.com

Gatan, Inc., Chad Tabatt

5933 Coronado Lane
Pleasanton, CA 94588
(925) 224-7318

Hamamatsu Photonic Systems

Butch Moomaw
360 Foothill Rd., Bridgewater, NJ 08807

JEOL (U.S.A.), Inc.

Richard Lois
256 Green Cove Drive
Montgomery, TX 77356
(409) 449-4141 FAX (409) 597-6200
lois@jeol.com/jlampert@jeol.com

KeveX/Fisons, Ed Terrell

5619 Tabletop Court
Boulder, CO 80301
(303) 530-3392
edt@keveX.com

LEICA Microsystems, Inc.,

Robert Seiler
2345 Waukegan Road
Bannockburn, IL 60015
(800) 248-0123,
www.leica-microsystems.com

M.E. Taylor Engineering, Inc.

SEM Division
21604 Gentry Lane
Brookeville, MD 208833
(301) 774-6246

Meyer Instruments

Rob Meyer
1304 Langham Creek, Suite 235
Houston, TX 77084
(281) 579-0342
www.meyerinst.com

Micro Star Technologies, Inc.

Cathy Ryan
511 FM 3179, Huntsville, TX 77340
(936) 291-6891 FAX (936) 294-9861
cathy.ryan@microstartech.com

Nikon Instruments Inc.

Mike Davis/Mike Johnson
1955 Lakeway Dr. Suite 250B
Lewisville, TX 75067
(888) 424-0880 FAX (888) 473-9511

Thermo NORAN

Bill Chauvin
2551 W. Beltline Hwy.
Middleton, WI 53562
(608) 836-4380 FAX (608) 836-7224
Cell (608) 347-7652
bill.chauvin@thermo.com
www.thermo.com/noran
Graham R. Bird
1021 Yellow Rose Drive
Salado, TX 76571-1035
(254) 947-8929
grbird@thegateway.net

NSA Hitachi, Kevin Cronyn

3109 Skyway Circle North,
Irving, TX 75038
(972) 257-8143 FAX (972) 257-8101
Kevin.Cronyn@hhta-hitachi.com

Oxford Instruments, Inc.

Mike Crowley/Theresa Jerszyk
3536 Flora Vista Loop,
Round Rock, TX 78681
crowley@ma.oxinst.com
jerszyk@ma.oxinst.com

Princeton Gamma-Tech, Inc.

Bob Green
458 Sherman Way, Decatur GA 30033
(404) 633-3904 FAX (404) 634-4587
beegreen@att.net

Rontec USA, Jessica Wheeler

20 Main Street, Acton, MA 01720
(978) 266-2900 FAX (978) 929-9313
wheeler@rontecusa.com

SCANNING/FAMS, Inc.

Mary K. Sullivan
P.O. Box 832, Mahwah, NJ 07430
(201) 818-1010 FAX (201) 818-0086
scanning@fams.org

Ted Pella, Inc., James Long

4595 Mountain Lakes Blvd.
Redding, CA 96003-1448
(512) 657-0898 FAX (530) 243-3761

Vital Image Technology, Steve Rapp

33811 Hanawalt Rd.,
Agua Dulce, CA 91350

ASSESSMENT OF AEROALLERGEN CONCENTRATION IN THE ATMOSPHERE OF THE TEXAS PANHANDLE USING A BURKARD VOLUMETRIC SPORE TRAP

NABARUN GHOSH¹, RENE CAMACHO¹, CONSTANTINE K. SAADEH² AND MICHAEL C. GAYLOR²

¹Department of Life, Earth and Environmental Sciences, West Texas A& M University, Canyon, TX 79016

²Amarillo Center for Clinical Research/ Allergy A.R.T.S. 6842 Plum Creek Drive, Amarillo, TX 79124

ABSTRACT

Airborne fungal spores and pollens are important allergens. Aeroallergens cause allergy to the sensitive people when come into contact with the eye or enter the body as the air is breathed. This study was intended to determine the composition of the major types of aeroallergens that are prevalent in the Texas Panhandle area and to detect possible correlation between the daily pollen and spore indices with the meteorological conditions. This study was done for two years (2002-2003).

Collection and transfer of the pollen sampling tape took place at the same time, 9:00 A.M. CDT. The analysis of air was performed through the collection of pollen and spores using a Burkard volumetric spore trap. To assess the daily aeroallergen concentration strips of Melinex tape were collected from the spore trap. The tapes were analyzed with a minimum of five latitudinal traverses, and daily concentration was assessed. The most significant aeroallergens present during this study were fungal spores from *Alternaria*, ascospores from Pezizales, *Dreschlera*, *Cladosporium*, *Curvularia*, and pollen from short ragweed (*Ambrosia artemisiifolia*), grass pollen (Poaceae) common sunflower (*Helianthus annuus*), hairy sunflower (*Helianthus hirsutus*), buffalo bur (*Solanum rostratum*), purple nightshade (*Solanum elaeagnifolium*) and lamb's quarters (*Chenopodium album*). The pollen and mold spore count varied with the meteorological conditions. There was a significant correlation between the numbers of patients' visits with the variation in spore index. Temperature was found to have an inverse relationship with mold spore concentration. Rainfall was found to affect the mold count directly, with increases in precipitation bringing subsequent higher mold spore concentrations. The number of reported cases of allergic rhinitis increased in proportion to the increases in overall allergen counts.

INTRODUCTION

Aeroallergens are often the cause of serious allergic and asthmatic reactions, affecting millions of people each year (1). Aeroallergen sampling provides information regarding the onset, duration, and severity of the pollen season that clinicians use to guide allergen selection for skin testing and treatment (2). To aid in the diagnosis and treatment of these individuals, a thorough understanding of the regional aerobiology is necessary. Weather conditions and diurnal cycles play an integral role in the passive and active discharge of spore and pollen. Dry weather promotes passive dispersal of dry air spores, including *Alternaria*, *Cladosporium*, *Curvularia*, *Pithomyces* and many smut teliospores. Moist weather conditions promote the active dispersal of moist air spores, such as the explosive release of ascospores from Pezizales, and the expulsion of basidiospores from the gills of the Basidiomycetes. In a given locale, the number of spores in the air fluctuates with prevailing conditions and is often particularly great after a rainfall, in part

because moisture is required for the effective operation of the spore discharge mechanisms (3). Often, the two most encountered mold spores in atmospheric sampling are ascospores from different species of Pezizales and spores from *Alternaria* sp. (4).

Ascospores are the sexual spores produced by Ascomyceteous fungi. Spores vary enormously in morphology, from single celled to multi-celled, from single septum to many septa. Because ascospores are released from the ascus through an active mechanism that requires moisture, they are frequently found when moisture levels are higher. *Alternaria* conidia are frequently the most abundant component of the dry air spores. In some areas, these asexual spores may be present throughout the year; however, peak concentrations usually occur in late summer or fall (5). Species of *Alternaria* are pathogens of a number of crop plants, causing wheat rust, early blight and black rots. Recent literature shows an association between *Alternaria* sensitivity and severe asthma (6).

This preliminary study includes a 2-year survey of the aeroallergen concentration in the air of the North-west Texas on a daily basis. It is also intended to detect possible relationship between the aeroallergen indices with both the meteorological and clinical data. The aeroallergen data were used to assess and evaluate the impact of airborne pollen and mold spores on the breathing and causes of allergic rhinitis in the susceptible individuals. This study was aimed to aid the diagnosis of allergic rhinitis by documenting the relation of pollen and fungal spore composition and concentration with the incidence of allergic rhinitis recorded in the Allergy Clinics at the Amarillo Center for Clinical Research.

MATERIALS AND METHODS

Trap preparation and allergen collection

The analysis of air was performed through the collection of pollen and spores through the use of the Burkard Volumetric Spore Trap (Burkard Agronomics Division of Burkard Scientific Sales Ltd., UK) (Fig. 1A). We standardized the Burkard Volumetric Spore Trap by using a flow meter provided by the manufacturer.

Preparation of the spore trap involves the removal of the collection drum from the collector and application of Melinex tape. This is accomplished through the measurement of Melinex tape to circumvent the drum. The Melinex tape is attached to the drum through the application of double-sided tape at the orifice start position (Fig. 1B). Once attached, the Melinex tape is coated with a thin layer of paraffin wax (Fisher Scientific cat #004 S8019WX) to adhere the pollen. This paraffin emulsion is comprised of a mixture of 18 grams paraffin wax, 150 ml (100g) petroleum jelly and 10 g phenol. It can be prepared beforehand and used as needed by melting in a water bath.

We mounted the spore trap on the flat roof of the Agriculture and Natural Sciences building of West Texas A&M University in Canyon, Texas. This area has adequate exposure to the prevailing

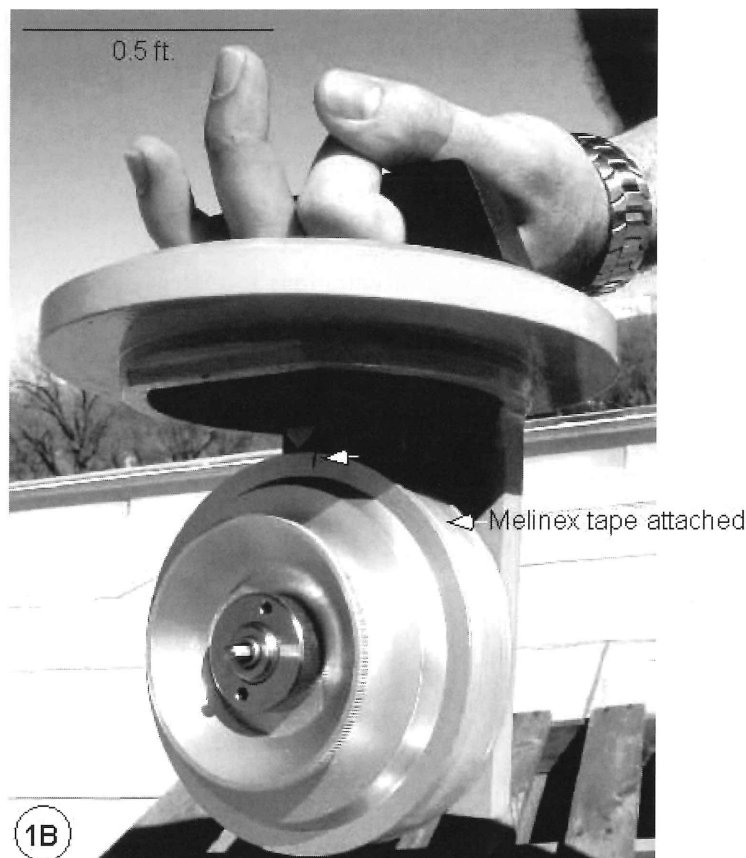
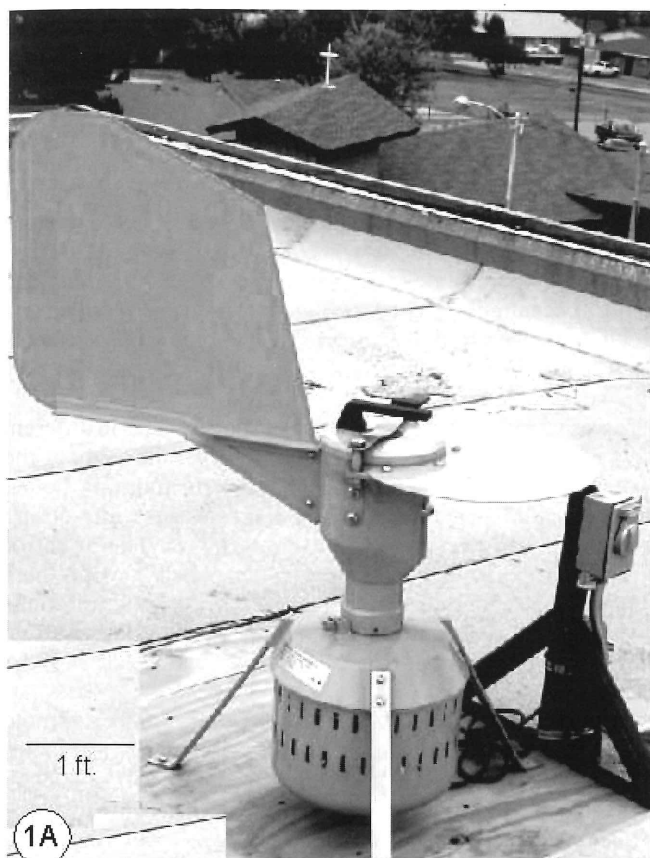


Figure 1A. Burkard Volumetric Spore Trap, 1B. Collection drum showing the orifice start position with an arrow pointing to it.

winds of West Texas, and is above the trees of the surrounding community. This location is beneficial because it allows adequate sampling of the wind-blown pollen and spores carried to the sampling apparatus on the air currents.

The spore trap operates on 25 watts of electricity at 240 volts, or 50 watts at 110 volts. Air is suctioned through the trap at a rate of 10 liters per minute. A fan on the ventral portion of the trap rotates at a rate of 2900 rpm to draw air into the trap. The complete rotation of the drum occurs over a seven-day period. Hourly observations can be made because the drum will rotate at a standard rate of 2 mm per hour. The distance from the beginning of the tape designates spore collection time (7).

A template is used to divide the tape into 24-hour periods. To assist in mounting, the template may be coated with a thin film of water to hold the tape in place. Segments of tape are cut from the drum to correspond with a twenty-four hour interval. These segments are then mounted on individual microscopic slides to be analyzed in 24-hour periods.

A clean microscopic slide is coated with a thin layer of water. The segment of tape is then laid upon the microscopic slide with the impregnated surface using forceps so that the long edges of the tape are parallel with the long edges of the slide. Positioning should be such that viewing of the entire slide may be accomplished from subsequent traverses of the slide. It is essential that the sides of the tape be mounted parallel to the sides of the slide so that traverses are to be truly traversed with the microscope.

The use of Gelvatol is required to secure the cover slip in place. This compound is applied with a glass rod and is a permanent mountant. Gelvatol is composed of 35 g Gelvatol powder (Burkard Manufacturing Co Ltd., UK), 50 ml Glycerol, 100 ml distilled water, and 2 g phenol. We prepared Gelvatol by mixing the Gelvatol

powder and phenol in water allowing sitting overnight. The mixture of phenol and Gelvatol was placed on a water bath (65°C) and glycerol and distilled water was added to it slowly while stirring produced the proper emulsion.

Upon distribution of the Gelvatol on the cover slip, a drop of Safranin O (Sigma Cat no. 84120, Fluka, Microscopy Grade) was placed upon the cover-slip and stirred evenly, when set on the slide it stained the pollen and spores facilitating the observation with a microscope. Safranin was prepared beforehand and stored in a glass bottle. We found 1% safranin was very effective stain in viewing pollen, including their cell walls and colpi (pores). The stain was comprised of 1.0 grams of Safranin O powder dissolved in a 50:50 mixture of 95% ethanol and distilled water. These components were dissolved in a round flask and were allowed to boil for 15-20 minutes. After cooling to the room temperature, this solution was filtered through Whatman's filter paper (Grade No. 43 Cat. no. 28481-302, 12.5 cm in diameter, VWR) into a second round flask. After filtering, the solution was transferred to glass vessels for long-term storage at room temperature.

Microscopic analysis of collected allergens

Sample tapes from the spore trap were analyzed regularly over the past two years (2002-2003). Collection and transfer of the pollen sampling tape took place at the same time, 9:00 A.M. CDT, on a daily basis. Tapes were analyzed with five latitudinal traverses corresponding to specific hours, and daily concentration was assessed. Daily mean concentrations were determined mathematically by taking a sum total of all traverses and multiplying this sum by a correction factor. Correction factors are microscope-objective specific and are determined prior to counting. It can be expressed as the total area sampled divided by the graticule width (7). The prepared slides were examined, counted, and photographed

using a BX-40 Olympus microscope attached to a DVC Camera. This assessment involved the optical counting of pollen grains and fungal spores through a microscope and the use of a micrometer scale and graticule (100 square micron). The graticule is a scale that measures distances to the 10^{-2} division of a millimeter. The graticule was calibrated using a stage micrometer. The pollen and fungal spores were identified using standard keys from literature and the websites (4, 5, 8, 9, 10, 11, 12).

Correlating the aeroallergen indices

To enable correlation of concentrations to meteorological conditions, weather data was recorded corresponding to the 24-hour interval analyzed. Information such as maximum daily temperature, minimum daily temperature, peak wind speed and daily precipitation were collected and compared with the aeroallergen indices and the numbers of patients visits at the clinic.

RESULTS AND DISCUSSION

The most significant allergens present during the period of June through September of 2002 and 2003 were the pollen from *Ambrosia artemisiifolia* (Short Ragweed)(Fig.2A), *Helianthus annuus* (Common Sunflower)(Fig. 2B), *Helianthus hirsutus* (Hairy Sunflower) (Fig. 2C), *Solanum rostratum* (Buffalo Bur) (Fig. 2D), *Solanum elaeagnifolium* (Purple Nightshade) (Fig. 2E), *Chenopodium album* (Lamb's Quarters) (Fig. 2F) and fungal spores of *Alternaria* sp. (Fig. 2G), *Stachybotrys* sp. (Fig. 2H), *Drechslera* sp. (Fig. 2I), *Curvularia* sp. (Fig. 2J), Ascospores, (Fig. 2K) and *Cladosporium* sp. (Fig. 2L). Significant increases in weed pollen, however, were observed in late August following several inches of rain. Fungal spore concentrations did show more susceptibility to meteorological conditions on a daily basis (Figs. 3C, 3D) than did pollen concentrations (Figs. 3A, 3C). High temperature reduced the weed pollen concentration whereas grass pollen concentration remained constant (Fig. 3A).

Of all the airborne pollen observed, the most significant was that of short ragweed (*Ambrosia artemisiifolia*). *Ambrosia* pollen is characterized by a spherical morphology with a multiporate surface and 16–27 micrometers in diameter (Fig.2A). Pores are geometrically arranged about the surface and can be seen easily using phase-contrast microscopy. *A. artemisiifolia* begins its pollination cycle in mid-August and continues until mid-October in the Texas Panhandle. Ragweed pollen is the largest single seasonal allergen in North America. One ragweed plant is capable of producing over a billion grains of pollen per season. In the United States, it is estimated that ragweed produces 100 million tons of pollen each year (13).

Grass (*Poaceae*) pollen was constant component of the pollen count through out the study, having peaks in mid-July and then again in late August. There are hundreds of different types of grass pollen that are typically encountered. Most grass pollen is similar in morphology, making identification of the species difficult without biochemical assays. Grass pollen has an ovate morphology with a single pore. Sizes range from 7 micrometers to over 75 micrometers, as in the case of corn (*Zea mays*) pollen. Significant smooth cell walls were observed on grass pollen, with little ornamentation being present on the surface (12).

Specifically, the mean concentration of tree pollen over the study period was 1.9-grains/cubic meter of air. The mean concentration of grass pollen was 8.0 grains /cubic meter of air, and of weeds the mean concentration was 35.2 ± 3.5 grains/cubic meter of air. For mold spores, the mean was 984.9 ± 6.2 spores/cubic meter of air over the study period. Mold spore concentration varied the most, followed by weed pollen. Tree pollen did not make up a significant amount of the overall pollen count. Weed pollen increased drastically in mid-August in both the years of study 2002 and 2003. Grass pollen concentrations remained steady throughout the season (Fig. 3A). The total pollen count inversely related to the wind speed

(Fig. 3B). Wind speed is a major factor controlling aeroallergen concentration in the Panhandle area.

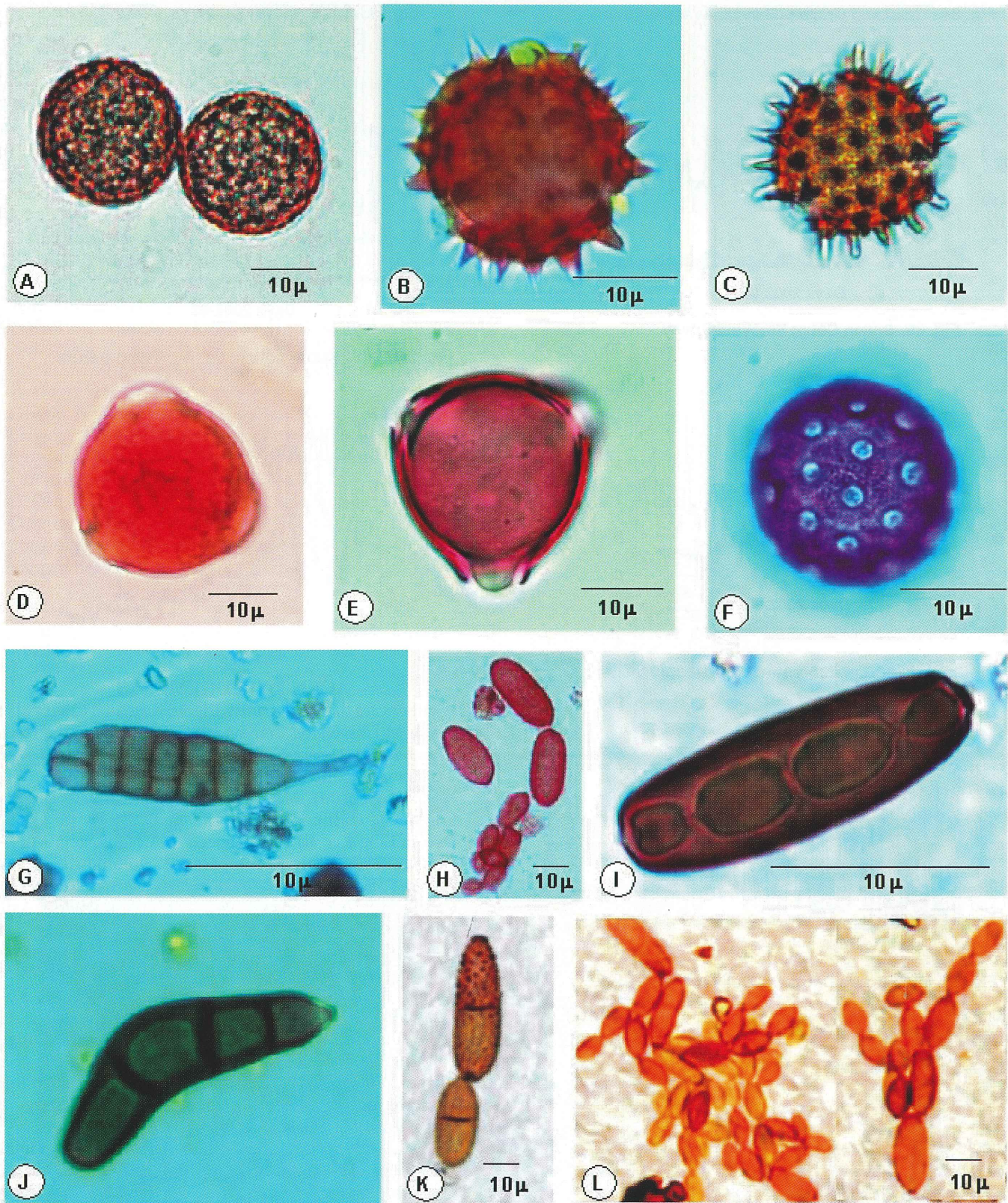
In comparison of collected pollen and spore data with weather information, it was revealed that specific weather variants could influence dispersal and concentration. The mean maximum temperature for this survey was $32.3 \pm 0.45^\circ\text{C}$, and the mean minimum temperature was $17.6 \pm 0.25^\circ\text{C}$. Temperature was found to have an inverse relationship with mold spores. As the temperature rose, mold spore concentrations would decrease throughout the day. Increase in temperature was observed to strongly reduce the ascospore concentration. With freezing temperatures the pollen and spore counts reached zero. We observed that the count of ascospores during wet weather could surpass the total concentration of dry conidia measured on a typical summer day.

There was variation in the occurrence of spore species in different times of the day. Ascospores, although observed throughout the day, were in greater concentration in the early morning hours. *Alternaria* conidiospores were present in greater quantities during the warmer, dryer afternoon and evening hours. The affect of temperature on pollen concentration is not as clear, though there does appear to be a long-term relationship. Temperature variations as they relate to seasonal changes have been shown to affect primarily the types of pollen observed, not necessarily the concentrations.

It was observed that precipitation increased the number of mold spores, but there was no direct correlation between number of spores and amount of rainfall. As noted earlier, certain genera of fungi, such as Ascomycetes, require raindrops to initiate their active dispersal mechanism. Corresponding to this knowledge, it was found that Ascomycetes concentrations significantly increased in the hours just following a rain shower. Precipitation in general affected mold spore concentrations directly by increasing the daily concentrations, due to increased relative humidity and to the availability of moisture (Fig. 3C). It was noted that in the hours just following precipitation, pollen concentrations were observed to drop drastically, as the particles were washed from the atmosphere.

Peak wind speed showed some direct correlation with mold spore or pollen concentrations. The mean peak wind speed over the study period was 5.4 m/s. It was observed that sustained windy or windless periods did have an effect on pollen and spore concentrations (Fig. 3B). Wind speeds over 8.0 m/s increased pollen and spore concentrations on average. Due to smaller size and less mass, mold spores were more directly influenced by wind speeds. Possibly a more representative comparison would be to compare average daily wind speed to the concentration of aeroallergens. Overall, the most prevalent aeroallergens present during the three-month interval where *Alternaria*, short ragweed (*Ambrosia artemisiifolia*) and grass (*Poaceae*) pollen. For the summer months that we observed, the most dominant pollen was grass (*Poaceae*), which peaked in July and then dropped off in August. In mid-August, the dominant pollen changed to ragweed (*Ambrosia artemisiifolia*), corresponding to the beginning of the flowering season for short ragweed (14).

The effect of aeroallergens on clinical patients was apparent. The number of reported cases of rhinosinusitis increased directly to the increases in overall allergen counts (Figs. 3E, 3F) as reported by us (18, 19) and the other workers (6,15,16). There was an increased incidence of pollinosis in Hakodate of Japan with allergic rhinitis caused by house dust and mite and pollen from *Artemisia*, grass (*Poaceae*) and *Cryptomeria japonica* (17). The number of patients visited the Allergy Clinic increased significantly with that of the increases in mold and *A. artemisiifolia* counts (Figs. 3E, 3F). Grass pollen was not as influential in cases presented to the clinic as weed pollen. The future objective of this study is intended to develop tools for forecasting aeroallergen index during different seasons of the year and to develop seasonal allergy indices specific for the Texas High Plains region.



Figures 2 A-L showing most frequent Aeroallergens of Texas Panhandle: **Pollens:**
 A. *Ambrosia artemisiifolia* (Short Ragweed), B. *Helianthus annuus* (Common Sunflower),
 C. *Helianthus hirsutus* (Hairy Sunflower), D. *Solanum rostratum* (Buffalo Bur),
 E. *Solanum elaeagnifolium* (Purple Nightshade), F. *Chenopodium album* (Lamb's Quarters).
Fungal spores: G. *Alternaria* sp. H. *Stachybotrys* sp. I. *Drechslera* sp. J. *Curvularia* sp.,
 K. Ascospores, L. *Cladosporium* sp.

Fig. 3A. Weed and Grass pollen vs. Av. temperature

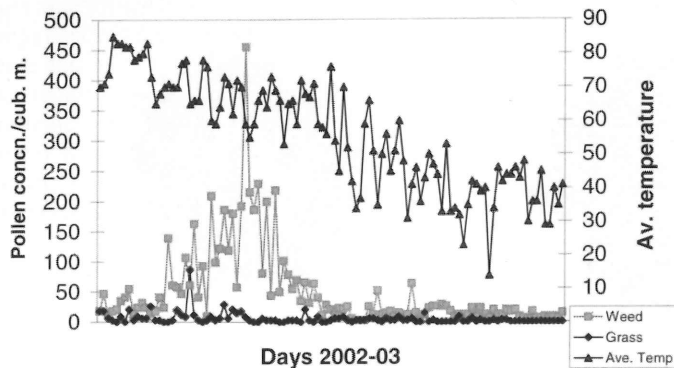


Fig. 3B. Pollen Count Vs. Wind Speed

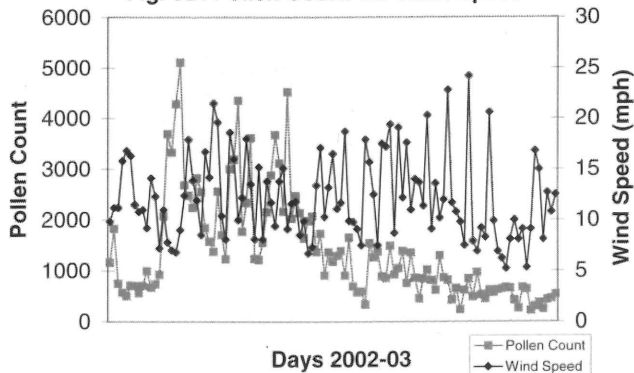


Fig. 3E Weed pollen count vs. Patients visit

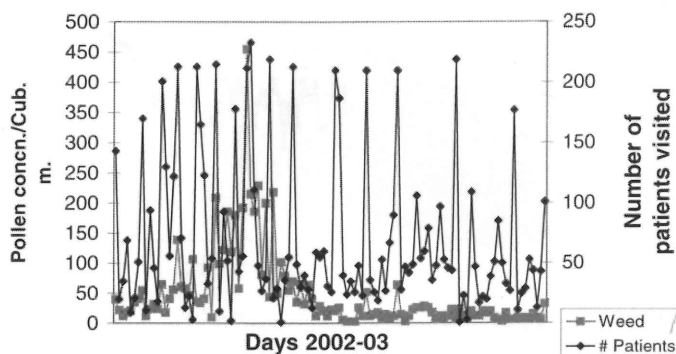


Fig. 3F. Mold Spore Count vs. Daily patient visit

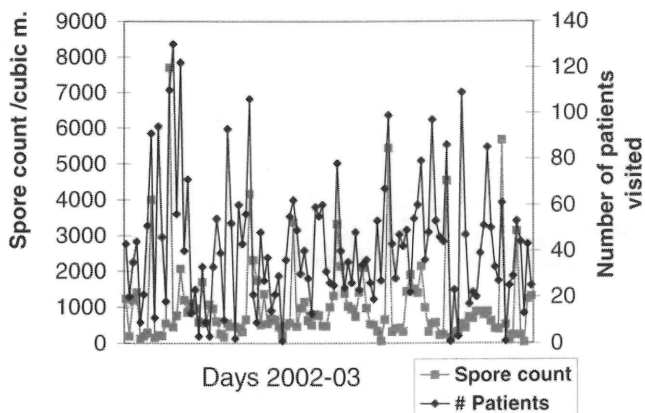


Fig. 3C. Mold spore concn. vs. Precipitation

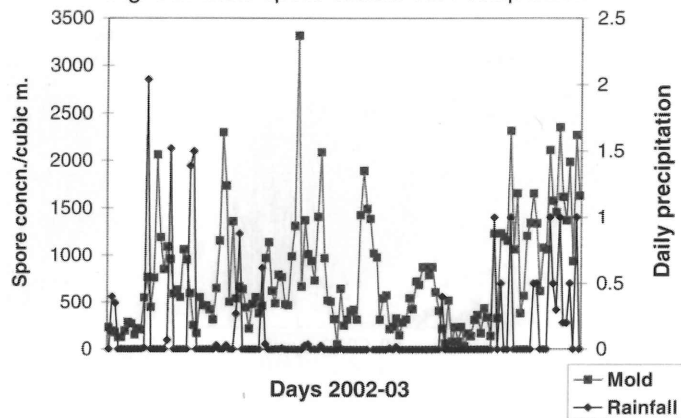
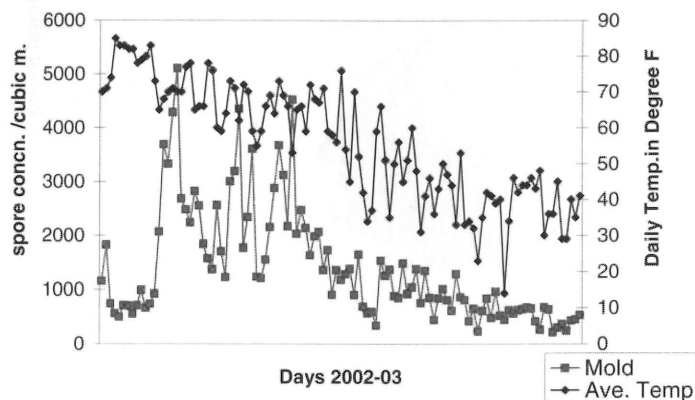


Fig. 3D. Mold spore concn. vs. Av. Temperature



ACKNOWLEDGEMENTS

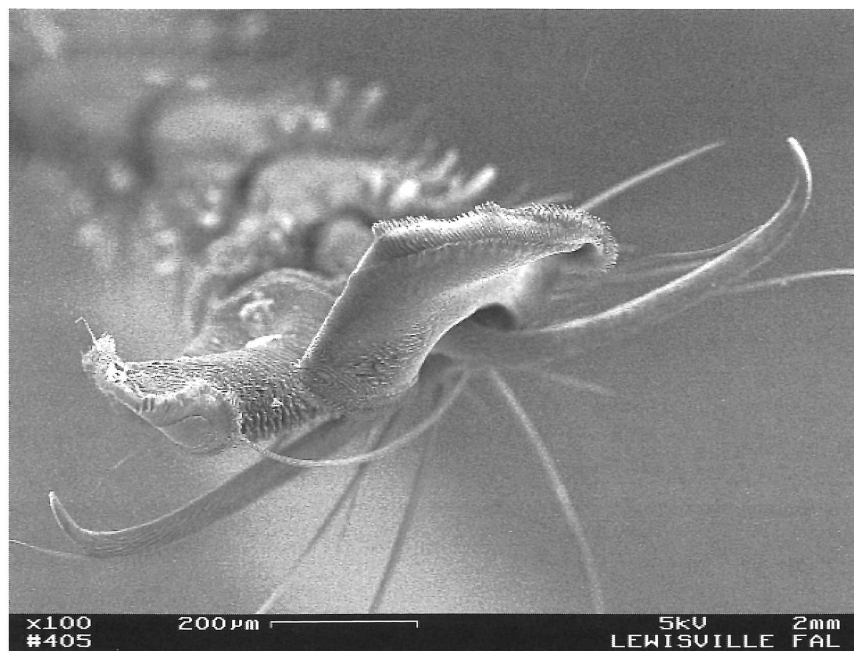
The authors are thankful to the Killgore Research Center of West Texas A & M University, Canyon for funding and to the research workers at the Amarillo Center for Clinical Research/ Allergy A.R.T.S. for collecting the clinical data.

1. Nester, E.W. 2001. Microbiology: A human perspective, 3rd Ed. McGraw-Hill, NY; pp. 1-15.
2. Dvorin D.J., Lee J.J., Belecanech G.A., Goldstein M.F., and Dunskey E.H. 2001. A comparative, volumetric survey of airborne pollen in Philadelphia, Pennsylvania (1991-1997) and Cherry Hill, New Jersey (1995-1997). *Ann Allergy Asthma Immunol* 87(5): 394-404.
3. Ingold, C.T. 1985. Water and spore discharge in ascomycetes and hymenomycetes. *Trans. Britt. Mycol. Soc.* 85: 575-583.
4. Ogden, E.C. 1974. Manual for Sampling Airborne Pollen, Hafner Press NY: 146-157.
5. Moore-Landecker, E. 1996. Fundamentals of the Fungi, 4th edition, Prentice Hall, NJ, pp. 342-343 and 400-401.
6. Skoner D.P. 2001. Allergic rhinitis: definition, epidemiology, pathophysiology, detection, and diagnosis, *J Allergy Clin Immunol* 108(1 Suppl.): S2-8.
7. Lacey, J. 1995. Airborne Pollens and Spores. A Guide to Trapping and Counting. The British Aerobiology Federation, U.K. pp. 1-59.
8. Horner, E., Levetin, E., Shane J.D., and Solomon, W. 2002. Advanced Aeroallergen. 58th AAAAI Annual Meeting, pp. 1-68.
9. Moore, P.D. 1991. Pollen Analysis, Second Ed. Blackwell Scientific Publications. Oxford, pp. 62-166.
10. American Academy of Allergy Asthma and Immunology: <http://www.aaaai.org/>
11. University of Arizona: <http://www.geo.arizona.edu/palynology/polonweb.html>
12. Jelks, M.L. 2002. Allergy Pollen Keys with Images. Sarasota, FL, pp. 1-19.

REFERENCES

13. Ragweed Pollen Allergy: <http://allergies.about.com/cs/ragweed/a/aa090699.htm>
14. Muilenberg, M. and Burge, H. 1996. Aerobiology. Lewis Publishers: Boca Raton, Florida, pp. 18-26.
15. Ito, Y., Kimura T., Miyamura T. 2002. Gramineae pollen dispersal and pollinosis in the city of Hisai in Mie Prefecture. A 14-year study of Gramineae pollen dispersal and cases of sensitization to Gramineae experienced at an allergy clinic over a 15-year period. *Arerugi*. 51(1): 9-14.
16. Narita S., Shirasaki H., Yamaya H., Mitsuzawa H., Kikuchi K., Kishikawa R., Kobayashi K., Himi T. 2001. The pollen survey and dynamic statistics of patients with allergic rhinitis in Hakodate. *Arerugi*. 50(5): 473-80
17. Narita S., Chin S., Shirasaki H., Takano Y., Kurose M., Kobayashi K., Kishikawa R., Koto E., Himi T. 2002. A study on the nasal and eye symptoms of pollinosis in Hakodate. *Arerugi*. 51(11):1103-12
18. Ghosh N., B. Patten, Lewellen, G. T., C. Saadeh, M. Gaylor. 2003. Aeroallergen survey of the Texas Panhandle using a Burkard Volumetric Spore Trap. *The Journal of Allergy and Clinical Immunology*. Vol. 111, No. 2: S91
19. Ghosh, N., R. Camacho, E. Schniederjan, C. Saadeh, M. Gaylor. 2003. Correlation between the meteorological conditions with the aeroallergen concentration in the Texas Panhandle. *Texas Journal of Microscopy*. 34:1:12-13

What Is It? *Answer In Next Edition*



SEM by Jodi A. Roeipsch,
Raytheon Network Centric
Systems, McKinney, Texas
75071.

High Resolution Sputter Coater 208HR



High Resolution Sputter Coater 208HR shown with Rotary-Planetary-Tilting Stage and Thickness Controller MTM-20
Fast coating with Turbo Vacuum for higher resolution requirements, such as FE-SEM

Superior Features

- **Wide Choice of Coating Materials**
Magnetron head design and effective gas handling allow a wide choice of target materials
- **Precision Thickness Control**
Thickness optimized to the FE-SEM operating voltage using the MTM-20 high resolution thickness controller
- **Multiple Sample Stage Movements**
Separate rotary, planetary and tilting movements allow optimized coating distribution and coverage
- **Variable Chamber Geometry**
Chamber geometry is used to adjust deposition rates from 1.0nm/sec to 0.002nm/sec to optimize structure
- **Wide Range of Operating Pressures**
Independent power / pressure adjustment allows operation at argon gas pressure ranges of 0.2-0.005mbar

- **Compact Modern Benchtop Design**

Space and energy saving design eliminates need for floor space, water, specialized electrical connections

Coating Difficult Samples for the FE-SEM

The High Resolution Sputter Coater 208HR offers solutions to the problems encountered when coating difficult samples for FE-SEM. In order to minimize the effects of grain size the 208HR offers a full range of coating materials and gives unprecedented control over thickness and deposition conditions. To minimize charging effects the 208HR stage design and wide range of operating pressures allows precise control of the uniformity and conformity of the coating. The HIGH/LOW chamber configuration allows easy adjustment of working distance.

 **TED PELLA, INC.**
Microscopy Products for Science and Industry



4595 Mountain Lakes Blvd., Redding, CA 96003-1448
Phone: 530-243-2200 or 800-237-3526 (USA) • FAX: 530-243-3761
Email: sales@tedpella.com • Web Site: <http://www.tedpella.com>



Performance and Precision *That Outshines The Competition*

The Histo Diamond Knife Family For Light Microscopy from

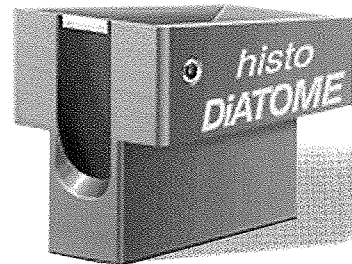
DiATOME

DiATOME Diamond Histo Knives outperform any other diamond knives on the market. They offer all of the outstanding characteristics desired from high quality diamond knives.

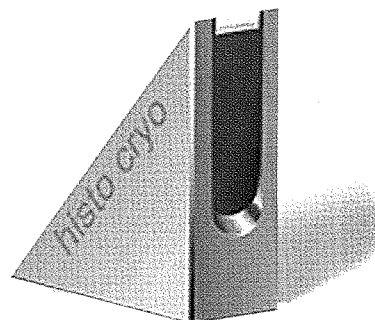
Outperform – *Easily cut perfect sections with less chatter or compression.*

Outlast – *Natural diamonds provide unparalleled durability and strength.*

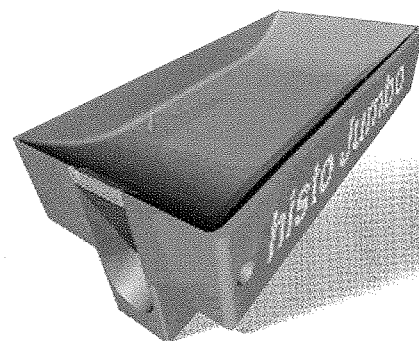
Outrank – *A distinct advantage over glass knives, diamond knives produce long ribbons of sections without knife making or knife changing.*



HISTO - for Plastic Embedded Specimens



CRYO-HISTO - for Frozen Specimens



JUMBO-HISTO - for Picking up Serial Sections



DiATOME
The ONLY Choice in High Quality Diamond Knives

Write or call today for information:

P.O. Box 125, 321 Morris Road, Fort Washington, PA 19034

TEL: (215) 646-1478 • FAX: (215) 646-8931

E-mail: sgkcck@aol.com • www.emsdiasum.com

APPLICATION FOR MEMBERSHIP OR CHANGE OF ADDRESS

TEXAS SOCIETY FOR MICROSCOPY, INC.

Date _____

Please type or print legibly. Fill out completely. The numbers in parentheses are the maximum number of characters and spaces the computer can accommodate for that blank. Though we will mail to your home address, we prefer to have your work address. Please note that membership is for Jan. - Dec. for each year.

Check One: ☐ I am applying for new membership in T.S.M.
☐ I am a member and wish to change my address.
☐ I am a STUDENT and wish to upgrade to REGULAR membership.

Are you a member of MSA? ☐ Yes ☐ No

Name (last name first) _____ (35)

Institution _____ (35)
(Please write out completely. We'll abbreviate it.)

Department _____ (35)
(Please write out completely. We'll abbreviate it.)

Street & Number / P.O. Box _____ (35)

City _____ (20) State _____ (2) Zip _____ (10)

Work Phone (_____) _____ (13) Extension _____ (4)

Electronic Mail (_____) _____ (40)

Home Phone (_____) _____ (13) FAX No. (_____) _____ (13)

Category of Membership (circle only one): **Regular** **Corporate** **Honorary** **Library**

Student: _____ Degree Program _____ Signature of faculty sponsor

Broad field of interest in which you utilize Microscopy (Circle only one):

Zoology
Medicine
Materials

Botany
Vet. Medicine
Petroleum

Microbiology
Chemistry
Semiconductor

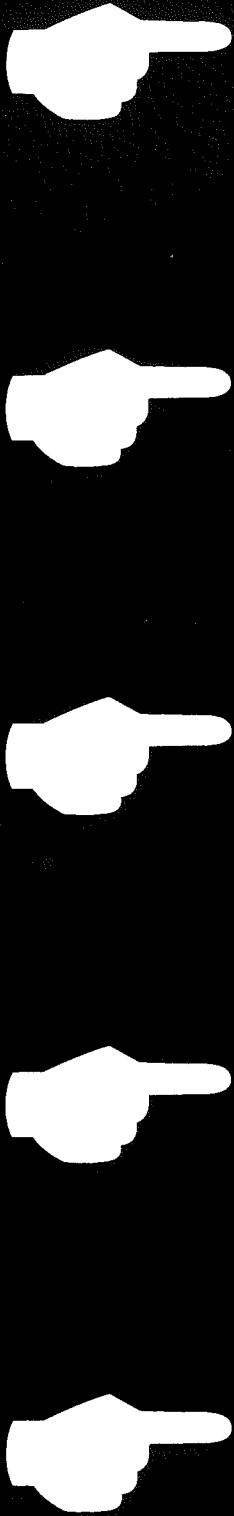
Cell Biology
Sales
Environment

Biochemistry
Service/Repair
Minerals

If you are a member changing your address, please attach an old mailing label to help us identify your previous record in the computer. Applicants for membership should include a check or money order for one year's dues with application (Regular: \$15.00; Student: \$2.00; Corporate: \$75.00).

Applications for new membership, or for upgrading of membership category from STUDENT to REGULAR, will be presented to the Executive Council at their next meeting for their approval (majority vote). The applicants will then be presented by the council to the membership at the next general business meeting for their approval (majority vote). Applicants will be added to the membership rolls at that time.

Please Return To: ROBERT CHAMPAIGN
Sensors and Electronic Systems
Raytheon Network Centric Systems
2501 W. University,
McKinney, Texas 75070
E-mail: r-champaign@raytheon.com



Lift 'n Press

Conductive Adhesive Tabs

For SEM Sample Preparation

Instant adhesion of SEM samples, just peel, press to apply to your sample mount, and lift off the paper backing.

Conductive adhesive, over 99% transparent to EDS.

Can be trimmed to accommodate any size mount.

Each roll contains 250 adhesive tabs

Part # CLNP \$29.95 per roll

**Call, Fax or E-mail:
M. E. Taylor Engineering, Inc**

21604 Gentry Lane

Brookville, MD 20833

Phone: (301) 774-6246

Fax: (301) 774-6711

E-mail: metengr@aol.com

visit us on the web

www.semsupplies.com

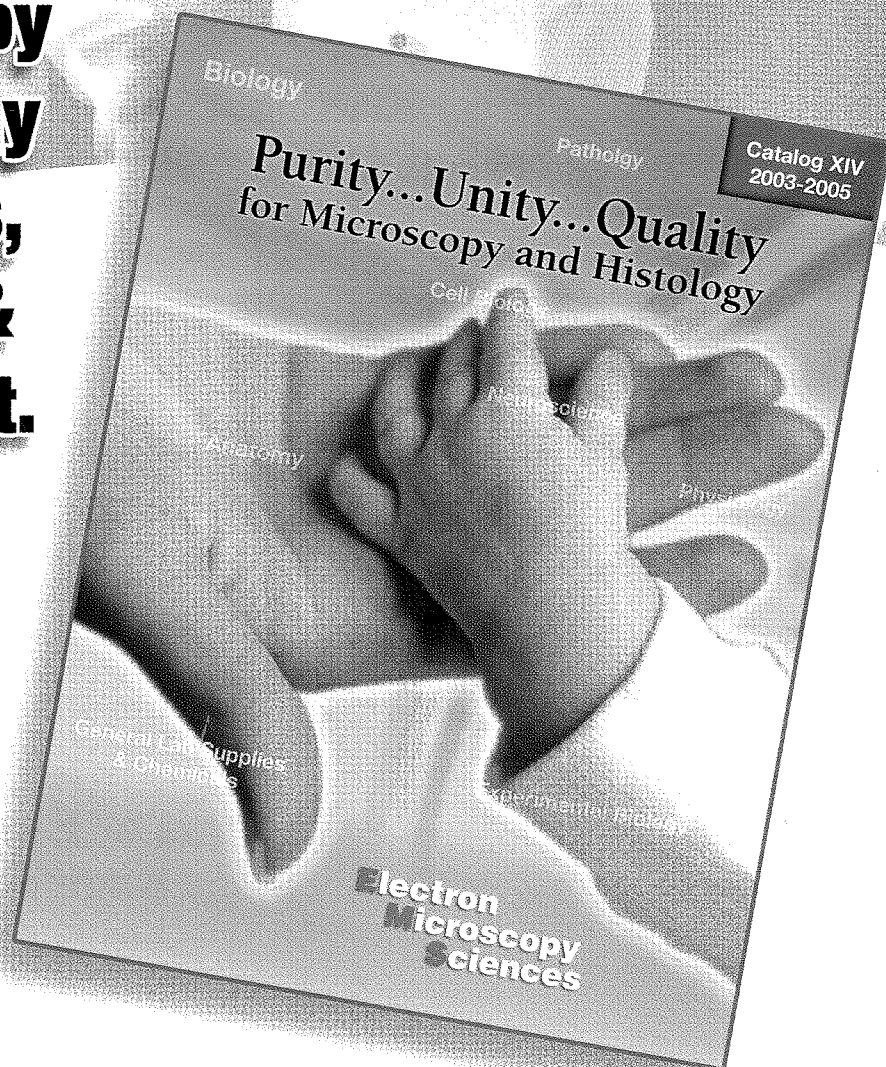
NEW

2003-2005 Catalog from EMS.

**The most comprehensive source for
microscopy
& histology
chemicals,
supplies &
equipment.**

Exacting
Research
Demands
High Quality
Products.

EMS is committed
to providing the
highest quality
products along with
competitive pricing,
prompt delivery and
outstanding customer service.



Call 800/523-5874 for your FREE catalog today!

**Electron
Microscopy
Sciences**

For more information and a complete catalog, write or call:
321 Morris Road, P.O. Box 251, Fort Washington, PA 19034
(215) 646-1566 • (800) 523-5874 • Fax (215) 646-8931
email: sgkcck@aol.com • <http://www.emsdiasum.com>